

# Nonequilibrium Dynamics of Symmetry Breaking in $\lambda\Phi^4$ Field Theory

Fred Cooper,<sup>1</sup> Salman Habib,<sup>1</sup> Yuval Kluger,<sup>2</sup> and Emil Mottola<sup>1</sup>

<sup>1</sup>*Theoretical Division, T-8, MS B285, Los Alamos National Laboratory, Los Alamos, NM 87545, USA*

<sup>2</sup>*Nuclear Science Division, Lawrence Berkeley National Laboratory, MS 70A-3307, Berkeley, CA 94720, USA*

(August 20, 2018)

The time evolution of  $O(N)$  symmetric  $\lambda\Phi^4$  scalar field theory is studied in the large  $N$  limit. In this limit the  $\langle\Phi\rangle$  mean field and two-point correlation function  $\langle\Phi\Phi\rangle$  evolve together as a self-consistent closed Hamiltonian system, characterized by a Gaussian density matrix. The static part of the effective Hamiltonian defines the True Effective Potential  $U_{eff}$  for configurations far from thermal equilibrium. Numerically solving the time evolution equations for energy densities corresponding to a quench in the unstable spinodal region, we find results quite different from what might be inferred from the equilibrium free energy “effective” potential  $F$ . Typical time evolutions show effectively irreversible energy flow from the coherent mean fields to the quantum fluctuating modes, due to the creation of massless Goldstone bosons near threshold. The plasma frequency and collisionless damping rate of the mean fields are calculated in terms of the particle number density by a linear response analysis and compared with the numerical results. Dephasing of the fluctuations leads also to the growth of an effective entropy and the transition from quantum to classical behavior of the ensemble. In addition to casting some light on fundamental issues of nonequilibrium quantum statistical mechanics, the general framework presented in this work may be applied to a study of the dynamics of second order phase transitions in a wide variety of Landau-Ginsburg systems described by a scalar order parameter.

PACS numbers: 03.70.+k, 05.70.Ln., 11.10.-z, 11.15.Kc

## I. INTRODUCTION

Spontaneous symmetry breaking by a scalar order parameter occurs in many different physical systems, as diverse as liquid  ${}^4\text{He}$  at temperatures of order  $2K$ , to the standard model of electroweak interactions at temperatures of order  $250\text{ GeV} = 3 \times 10^{15}K$ . The prototype renormalizable quantum field theory describing this symmetry breaking is a scalar field with a  $\lambda\Phi^4$  self-interaction. The behavior of the finite temperature effective potential or Landau-Ginsburg-Helmholtz free energy in this theory is well-known and forms the usual basis for discussion of the symmetry restoration at high temperature. On the other hand, surprisingly little effort has been devoted to the nonequilibrium or time dependent aspects of the symmetry breaking phase transition. With the development of practical general techniques for studying time dependent problems in quantum field theory, as well as the advent of high speed supercomputers it has become possible to address these dynamical issues systematically for the first time. It is clear that a detailed description of the time dependent dynamics will be necessary to calculate nonequilibrium properties of the phase transition, such as the formation and evolution of defects in the  ${}^4\text{He}$  system after a rapid quench, or the efficiency of baryogenesis in the electroweak phase transition. Other examples requiring the detailed time evolution of scalar fields are the chiral phase transition of the strong interactions such as may soon be probed in relativistic heavy-ion colliders and the problem of reheating

the very early universe after it has passed through an epoch of rapid expansion and cooling.

All of these problems require a consistent treatment of time-dependent mean fields such as the scalar expectation value  $\langle\Phi\rangle$  in interaction with its own quantum and/or thermal fluctuations. The technique we rely upon in this paper consists of replicating the scalar field  $\Phi \rightarrow \Phi_i, i = 1, \dots, N$ . Then it becomes possible to compute the quantum effective action in a systematic power series in the parameter  $1/N$  [1]. Variation of this effective action yields equations of motion for the mean fields coupled to Green’s functions of the theory which are suitable for implementation on a computer. The leading order in large  $N$  corresponds to a self-consistent mean field approximation, *i.e.* a truncation of the infinite hierarchy of Schwinger-Dyson equations for the  $n$ -point correlation functions to a closed Hamiltonian system of just the one-point function,  $\langle\Phi(x)\rangle$  and two-point function,  $\langle\Phi(x)\Phi(x')\rangle$ . Because no irreducible correlators higher than these appear in the leading order of the large  $N$  expansion, it is equivalent to a Gaussian approximation to the time-dependent density matrix of the system. As will become apparent, the approximation allows automatically for a mixed-state Gaussian density matrix,  $\rho$ , and is therefore more general than a Gaussian ansatz for the pure state wave function in the Schrödinger picture. Hence, the mixed-state Gaussian width of  $\rho$  can describe at once and on the same footing both the quantum and classical statistical fluctuations of the  $\Phi$  field about its mean value far from thermal equilibrium.

An important property of the evolution equations in the large  $N$  limit is that they are Hamilton's equations for an effective *classical* Hamiltonian  $H_{eff}$  (in which  $\hbar$  appears as a parameter). This effective Hamiltonian turns out to be nothing else than the expectation value of the full quantum Hamiltonian  $\mathbf{H}$  in the general mixed state described by the time-dependent Gaussian density matrix,  $\rho$ , *i.e.*,

$$H_{eff} = \text{Tr}(\rho\mathbf{H}) . \quad (1.1)$$

The canonical variables of  $H_{eff}$  are in one-to-one correspondence with the parameters needed to specify the general Gaussian density matrix in the Schrödinger picture, or the one- and two-point functions of the Schwinger-Dyson hierarchy in the Heisenberg picture. In order to highlight the Hamiltonian structure of the mean field equations, our first purpose in this paper will be to establish these various correspondences in detail for the  $O(N)$  symmetric  $\lambda\Phi^4$  theory. The existence of an effective Hamiltonian makes it clear from the outset that the leading order large  $N$  approximation is self-consistent and energy conserving, and hence does not introduce any time irreversibility or dissipation “by hand” into the system.

A corollary of the identification of the effective Hamiltonian  $H_{eff}$  in the large  $N$  limit is that its static piece  $U_{eff}$  (obtained by setting all the canonical momenta to zero) is the *True Effective Potential* which governs the nonequilibrium evolution of the system. This True Effective Potential (TEP) is real, and completely well-defined for states far from thermal equilibrium. In the special case of thermal equilibrium it becomes the *internal* energy  $U$  of the closed Hamiltonian system described by  $H_{eff}$ . In contrast, the Helmholtz free energy  $F$  which is sometimes called the “effective” potential is not defined away from thermal equilibrium and becomes complex in the unstable spinodal co-existence region between the two spontaneously broken vacua in simple approximation schemes. This is easily understood in the more general nonequilibrium context of this paper: it means simply that there is no stable equilibrium state in the co-existence region with a fixed constant value of  $\langle\Phi\rangle$ . In other words, if we start at  $t = 0$  with initial conditions corresponding to this putative thermal equilibrium state, the system immediately begins to evolve in time away from it, and this is the physical meaning of the imaginary part of  $F$  [2].

We shall see that the free energy function  $F$  (or simply its real part) is a very poor guide to the time evolution of the system far from thermal equilibrium. In particular, the oscillations of the time dependent expectation value  $\langle\Phi\rangle(t)$  about the spontaneously broken minima are characterized by a frequency (the plasma frequency) which is *not* the second derivative of  $F$  at its minimum (which turns out to be zero), and moreover, even the *location* of the minima of  $F$  is in general different from the stationary points of the mean field evolution. Explicitly

solving for the actual nonequilibrium mean field dynamics and demonstrating that it is quite different from what might be inferred from an uncritical use of the equilibrium free energy function  $F$  is the second major emphasis of this work. In this we corroborate the similar conclusions reached in Ref. [3].

The spontaneous breakdown of the global  $O(N)$  symmetry in the model leads to the existence of  $N - 1$  massless Goldstone bosons (in  $d > 1$  spatial dimensions), which dominate the dynamics in the large  $N$  limit. In  $d \leq 1$  spatial dimension there is no symmetry breaking and the system is inevitably driven into the symmetric phase, no matter what the initial state or energy density. The one dimensional case is of more than passing interest in showing how the  $O(N)$  symmetry is restored dynamically and the Mermin-Wagner-Coleman theorem [4] is satisfied in real time. For  $d > 1$ , the absence of a finite mass threshold means that an arbitrarily small amount of energy in the mean field can create massless Goldstone boson pairs nearly at rest. This open channel provides an efficient mechanism for the mean field to continuously transfer its kinetic energy to the massless particle modes over time. The presence of a symmetry which requires massless particles is a feature which the  $O(N)$  model shares with other physically interesting theories such as non-abelian gauge theories and gravity. The  $O(N)$  scalar theory provides an instructive example of dissipation by means of massless particle creation, which should be applicable in other quite diverse contexts, such as gluon production in relativistic heavy-ion collisions or graviton creation in early universe phase transitions. Developing techniques and gaining some valuable intuition for these more challenging problems is our third reason for presenting a study of massless  $\lambda\Phi^4$  theory in some detail.

It is remarkable that despite the explicitly Hamiltonian structure of the mean field equations, we observe quasi-dissipative features in the evolution, in the sense that energy flows from the mean field  $\langle\Phi\rangle$  into the fluctuating particle modes without returning over times of physical interest. In other words, although the underlying equations are fully time-reversal invariant, typical evolutions beginning with energy concentrated in the mean fields are *effectively irreversible*, at least over very long intervals of time. This apparent irreversibility is quantifiable first, in terms of the increase in particle entropy obtained by averaging over the rapidly varying phases of the fluctuating modes, and second, by the effective damping rate of the collective motion which we calculate by a standard linear response analysis. Since the mean field Gaussian approximation contains no collision terms, the particles interacting with each other only through the mean fields, this effective relaxation to a quasi-stationary (but non-thermal) state is a form of collisionless damping, similar to Landau damping in non-relativistic electromagnetic plasmas. We call this collisionless damping due to effective loss of phase information in the fluctuating quantum modes *dephasing*. Dephasing of the fluctuations is both an ex-

tremely general and efficient mechanism for introducing effective dissipation into the reversible Hamiltonian dynamics of mean field evolution. Hence, even in this relatively simple collisionless approximation to a quantum many-body theory one can begin to see how irreversibility and the second law of thermodynamics emerge from a consistent treatment of fluctuations in a closed Hamiltonian system. Collisions which first appear at one order beyond the mean field limit in the large  $N$  expansion would be expected to make the dephasing and dissipation found at lowest order still more efficient.

In addition to the effective dissipation of energy from the collective plasmon mode to the fluctuations, dephasing is also responsible for quantum decoherence, in the sense of suppression with time of the off-diagonal elements of the Gaussian density matrix. The point is that by going to the appropriate time-dependent number basis the diagonal matrix elements of  $\rho$  are adiabatic invariants of  $H_{eff}$  and therefore slowly varying functions of time, while the off-diagonal elements are very rapidly varying. These rapid phase variations in the off-diagonal interference terms cancel out very efficiently when the sum over the mode momentum is performed, or if the phases in a given mode are averaged in time. In either case, the particle creation and interactions have the effect of bringing the quantum system into what *effectively* looks more and more nearly like a classical mixture in which the phase information in the off-diagonal components may be discarded for most practical purposes at late times. The symmetry breaking behavior of the density matrix and effective disappearance of quantum interference between the two classically allowed outcomes is the final result. An important consequence of decoherence is the appearance of a diagonal effective density matrix which may be sampled to generate smooth classical field configurations. These configurations are free from spurious cut-off dependences and can be used to address issues such as the generation of topological defects in a nonequilibrium phase transition and the modeling of individual events in heavy-ion collisions.

The time-dependent scalar theory is an excellent theoretical laboratory for the study of general nonequilibrium phenomena such as decoherence and the quantum to classical transition quite aside from specific potential applications to phase transitions in many systems of physical interest. The detailed study of effective dissipation and decoherence in an explicit field theoretic example is the fourth major focus of the present work. Some of our results on the Hamiltonian nature of the evolution and on dephasing and decoherence have been reported earlier in condensed form [5].

The paper is organized as follows. In the next Section we begin by reviewing the large  $N$  expansion of  $\lambda\Phi^4$  theory in the real time effective action formulation. Then the Hamiltonian structure of the equations of motion is exhibited and the effective Hamiltonian and Gaussian density matrix are identified in Section III. The static part of this effective Hamiltonian is the nonequilibrium

True Effective Potential (TEP),  $U_{eff}$  which we define and relate to the thermodynamic free energy  $F$  in Section IV. Numerical evolution of the actual equations of motion in both one and three dimensions show clearly the difference with what might have been inferred from  $F$ . In Section V we identify the adiabatic particle number basis in which dissipation through the increase of the effective particle entropy and decoherence are described. We also present numerical evidence for the efficient dephasing of the quantum modes in the time-dependent mean fields, and show how it leads to typical classical configurations in the mixture in which quantum interference effects have been washed out. In Section VI we perform a linear response analysis of small perturbations away from thermal equilibrium, as well as away from the non-thermal stationary states found in the previous sections, compute the plasmon damping rate, and compare it with the numerical results. There is excellent agreement in the thermal case for both the plasmon frequency and damping rate, whereas the non-thermal situation is more complicated. We conclude in Section VII with a discussion of our results and of their possible application to diverse problems of interest in the real time dynamics of second order phase transitions with a scalar order parameter. There are three Appendices, the first on the renormalization of the energy and pressure of the theory, the second cataloguing some mathematical properties of the Gaussian density matrix used in the text, and the third containing the details of the numerical methods used in solving the equations.

## II. THE LARGE $N$ EFFECTIVE ACTION

The most direct method of deriving the equations of motion in the large  $N$  approximation is the method of the effective action, which also has the advantages of exhibiting the covariance properties of the theory explicitly and providing a general framework for the systematic expansion in powers of  $1/N$  to any desired order beyond the mean field approximation. Here we will present a short derivation of the effective action and refer the interested reader to the earlier work [1] for details of the derivation, which is quite standard. The underlying  $O(N)$  symmetric scalar field theory with which we begin is described in  $d$  space dimensions by the classical action,

$$\begin{aligned} S_{cl}[\Phi, \chi] &= \int dt d^d x L_{cl}[\Phi, \chi] \\ &= \int dt d^d x \left\{ -\frac{1}{2} \Phi_i G^{-1}[\chi] \Phi_i + \frac{N}{\lambda} \chi \left( \frac{\chi}{2} + \mu^2 \right) \right\} \end{aligned} \quad (2.1)$$

where  $i = 1, \dots, N$  and

$$G^{-1}[\chi] \equiv -\square + \chi, \quad (2.2)$$

with the metric signature  $(-, +, +, +)$ . This form of the action is equivalent to the more familiar Lagrangian density,

$$\begin{aligned}\tilde{L}_{cl}[\Phi] &= -\frac{1}{2}(\partial_\mu\Phi_i)(\partial^\mu\Phi_i) - V_{cl} \\ &= -\frac{1}{2}(\partial_\mu\Phi_i)(\partial^\mu\Phi_i) - \frac{\lambda}{8N}\left(\Phi_i\Phi_i - \frac{2N\mu^2}{\lambda}\right)^2\end{aligned}\quad (2.3)$$

with the definition of the auxiliary field  $\chi$  by

$$\chi = -\mu^2 + \frac{\lambda}{2N}\Phi_i\Phi_i, \quad (2.4)$$

since the two Lagrangians  $L_{cl}$  and  $\tilde{L}_{cl}$  are then equal up to a surface term. The quartic coupling in the Lagrangian has been taken to be  $\lambda/N$  from the outset, rather than rescaling it later by  $1/N$  as is sometimes done [6].

If the parameter  $\mu^2 > 0$ , then this classical Lagrangian describes spontaneous symmetry breaking since the minimum of the classical potential  $V_{cl}$  occurs at

$$\Phi_{i\text{ vac}} = \delta_{iN} v_0 \sqrt{N} \quad ; \quad v_0 = \sqrt{\frac{2}{\lambda}} \mu \quad (2.5)$$

rather than at zero. The second derivative of the classical potential at its minimum is

$$\begin{aligned}\frac{\partial^2 V_{cl}}{\partial\Phi_i\partial\Phi_j} &= \frac{\lambda}{2N}\left(\Phi_k\Phi_k - \frac{2N\mu^2}{\lambda}\right)\delta_{ij} + \frac{\lambda}{N}\Phi_i\Phi_j \\ &= \left(\chi\delta_{ij} + \frac{\lambda}{N}\Phi_i\Phi_j\right) \\ &= \begin{cases} 0, & i \text{ or } j = 1, \dots, N-1 \\ \lambda v_0^2, & i = j = N. \end{cases}\end{aligned}\quad (2.6)$$

At this minimum the  $O(N)$  symmetry is spontaneously broken,  $\chi = 0$  and there are  $N-1$  massless modes. Small oscillations in the remaining  $i = N$  direction describe a massive mode with bare mass equal to  $\sqrt{2}\mu = \sqrt{\lambda}v_0$ . In this standard way of describing the symmetry breaking, one direction is singled out and its vacuum expectation value is scaled with  $\sqrt{N}$  as in (2.5). It is clear that in the large  $N$  limit the effects of this single degree of freedom are down by  $1/N$  compared to the  $N-1$  massless modes which dominate the dynamics. As we shall see in Section VII the effects of the single massive degree of freedom are recovered in the behavior of the  $\chi$  correlator at late times.

Passing now to the quantum theory, the large  $N$  mean field approximation is obtained by retaining only the leading terms in a systematic expansion of Feynman diagrams in  $1/N$ . To lowest order, the quantum effective action is

$$\mathcal{S}_{eff}[\phi, \chi] = N\mathcal{S}_{cl}[\phi, \chi] + N\frac{i\hbar}{2}\text{Tr}\ln G^{-1}[\chi]. \quad (2.7)$$

We use units in which the speed of light and Boltzmann's constant are unity,  $c = k_B = 1$ , but we retain  $\hbar$  in order

to exhibit the semiclassical nature of the large  $N$  limit. The effective action,  $\mathcal{S}_{eff}$  generates the proper vertices of the  $O(N)$  symmetric  $\lambda\Phi^4$  theory, correct to leading order in  $1/N$ . It is just  $N$  times the classical action for a *single* component  $\phi$  field, plus the self-consistent (or resummed) one-loop correction represented by the last  $\text{Tr}\ln G^{-1}[\chi]$  term, where  $\chi$  is the mass squared of the propagator  $G$  appearing in the loops. The quantity  $\phi \equiv \langle\Phi\rangle$  is the mean value of the quantum field  $\Phi$ . Thus, in this description we effectively return to a single component  $\Phi^4$  theory. The role of the large  $N$  limit is to justify the neglect of the single massive degree of freedom relative to the  $N-1$  massless Goldstone bosons in the propagator  $G[\chi]$  of the  $\Phi$  field. However, the massive degree of freedom determines the  $\chi$  propagator which controls the plasmon oscillations discussed in Section VI.

Before proceeding it is worth pausing at this point to compare and contrast the large  $N$  effective action (2.7) with two different but related approximations. The simplest is the standard one-loop approximation on the single component theory, which is obtained by expanding the  $\Phi$  field about its mean value  $\phi$ . The quantum effective action in this approximation is

$$\mathcal{S}_{1-loop}[\phi] = \tilde{\mathcal{S}}_{cl}[\phi] + \frac{i\hbar}{2}\text{Tr}\ln G^{-1}[V_{cl}''] \quad (2.8)$$

where the effective mass appearing in the two-point function is

$$V_{cl}'' = \left.\frac{\partial^2 V_{cl}}{\partial\Phi^2}\right|_{\Phi=\phi} = -\mu^2 + \frac{3\lambda}{2}\phi^2. \quad (2.9)$$

The simple one-loop approximation includes only the one-loop self-energy diagram of Fig. 1, without any further resummation of diagrams.

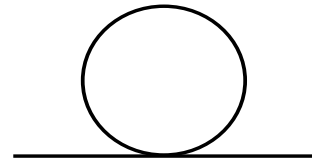


FIG. 1. The one-loop self-energy diagram which contributes to the simple one-loop effective action of Eqn. (2.8).

In contrast, the approximation usually called the Hartree or Gaussian approximation in the literature is closely related to the large  $N$  approximation in that the second derivative of the classical potential  $V_{cl}''$  in (2.8) is replaced by its Gaussian mean value, *viz.*

$$\mathcal{S}_{Hartree}[\phi, M^2] = \mathcal{S}_{cl} + \frac{i\hbar}{2}\text{Tr}\ln G^{-1}[M^2] \quad (2.10)$$

with

$$M_{ij}^2 \equiv \left\langle\frac{\partial^2 V_{cl}}{\partial\Phi_i\partial\Phi_j}\right\rangle = \langle-\mu^2 + \frac{\lambda}{2N}\Phi_k\Phi_k\rangle\delta_{ij} + \frac{\lambda}{N}\langle\Phi_i\Phi_j\rangle. \quad (2.11)$$

In the Hartree approximation the classical action should be expressed in terms of the set of variational parameters,  $\phi$  and  $M_{ij}^2$ . In both the Hartree and large  $N$  approximations the expectation values of bilinears obey the factorization condition,

$$\langle \Phi_i(x) \Phi_j(y) \rangle = \langle \Phi_i(x) \rangle \langle \Phi_j(y) \rangle - i\delta_{ij}G(x, y), \quad (2.12)$$

where which two-point function  $G$  appears here depends on the application. In any case, this factorization implies that the last term in (2.11) above is suppressed by a factor of  $1/N$  compared to the diagonal  $\delta_{ij}$  term. The difference between the Hartree and large  $N$  effective action is just this last term in (2.11). In the large  $N$  approximation it is discarded at leading order as in (2.6) and (2.7), whereas in the Hartree approximation of Eqns. (2.10) and (2.11) it is retained. An important consequence of this difference between the two approximation schemes is that unlike the Hartree approximation, the large  $N$  effective action is the leading term in a series in a well-defined expansion in powers of  $1/N$ . Thus, it is possible to improve on the large  $N$  limit in a systematic way by retaining higher order terms in this series. In contrast, the Hartree approximation is simply a variational ansatz.

In addition to providing a practical expansion technique the large  $N$  expansion has the significant conceptual advantage over the Hartree approximation of placing mean field theory in its proper context with respect to other systematic methods in nonequilibrium statistical mechanics. In fact, the systematic truncation of the Schwinger-Dyson hierarchy of connected  $2n$ -point functions by the large  $N$  expansion in quantum field theory is the precise analog of the truncation of the BBGKY hierarchy of  $n$ -particle distribution functions in nonequilibrium classical statistical mechanics. The existence of an energy-conserving expansion parameter in  $1/N$  which preserves all the relevant symmetries of the underlying field theory is a powerful technical tool for development of the quantum theory of nonequilibrium processes from first principles in a systematic way.

The effective mass which appears in the large  $N$  effective action is

$$\begin{aligned} \chi(x) &= \langle -\mu^2 + \frac{\lambda}{2N} \Phi_i(x) \Phi_i(x) \rangle \\ &= -\mu^2 + \frac{\lambda}{2} \phi^2(x) - \frac{i\lambda}{2} G[\chi](x, x) \end{aligned} \quad (2.13)$$

which will be recognized as just the expectation value of the (operator) definition of the auxiliary field in (2.4) upon using the factorization condition (2.12). Since  $G[\chi]$  itself depends on  $\chi$  through the definition,

$$\begin{aligned} G^{-1}[\chi] \circ G[\chi] &= 1 \quad \text{or} \\ (-\square + \chi) G[\chi](x, y) &= \delta^{d+1}(x - y) \end{aligned} \quad (2.14)$$

in position space, (2.13) is a nonlinear integral equation for the auxiliary field  $\chi$ . The Feynman diagrams that contribute in both the large  $N$  limit and the Hartree approximation are the sum over all daisy and superdaisy

diagrams represented in Fig. 2, with the only difference that the lines correspond to the propagator  $G[\chi]$  in one case (large  $N$ ) and  $G[M^2]$  in the other case (Hartree). This is just the resummation of self-energy diagrams required by a renormalization group analysis, and in fact,  $\chi$  is a renormalization group invariant. In the large  $N$  limit the fundamental excitations are the  $N-1$  Goldstone modes, whose masslessness is fixed by the  $O(N)$  symmetry which the  $1/N$  expansion respects order by order. In contrast, since the Hartree approximation is not a systematic expansion in any small parameter it is not clear *a priori* how to renormalize  $M^2$ , nor whether it has any renormalization group invariant meaning. The result is that although the two approximations are very similar in some respects and may be handled by the same techniques, the physics they describe is really quite different. Which approximation is more reliable depends very much on the application, and in particular whether or not the massless Goldstone modes of the large  $N$  limit actually play the lead role in the physics we wish to describe.

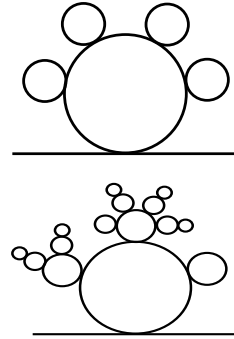


FIG. 2. Typical daisy and superdaisy diagrams included in the Hartree or leading order large  $N$  approximation to the effective action.

In the real time formulation, the effective action of (2.7) becomes the starting point for all further analysis of the large  $N$  dynamics. From the construction of  $\mathcal{S}$  in (2.7) as a Legendre transform in the presence of external sources, it follows that its first variation with respect to the independent mean fields  $\phi$  or  $\chi$  is proportional to the sources for these fields. In the absence of external sources, these variations yield the equations of motion for the mean fields,

$$\frac{1}{N} \frac{\delta \mathcal{S}_{eff}[\phi, \chi]}{\delta \phi} = G^{-1}[\chi] \phi(x) = (-\square + \chi(x)) \phi(x) = 0, \quad (2.15)$$

and

$$\begin{aligned} \frac{1}{N} \frac{\delta \mathcal{S}_{eff}[\phi, \chi]}{\delta \chi} &= \frac{(\chi(x) + \mu^2)}{\lambda} - \frac{1}{2} \phi^2(x) + \frac{i\hbar}{2} G[\chi](x, x) \\ &= 0, \end{aligned} \quad (2.16)$$

which just recovers (2.13) to this order. Unlike the equation (2.15) for  $\phi$ , (2.16) involves no derivatives and is

therefore an equation of constraint (or gap equation), rather than an equation of motion for an independent propagating degree of freedom. That  $\chi$  is nevertheless a useful indicator of symmetry breaking should be clear from the spacetime independent form of Eqn. (2.15),

$$\chi\phi = 0, \quad (\partial_\mu\phi = 0) \quad (2.17)$$

which tells us that either  $\phi$  or  $\chi$  (or both) must vanish in a uniform, stationary state. The case,  $\phi = 0$  is the  $O(N)$  symmetric state with generally positive  $\chi$ , while the case of non-vanishing  $\phi$  is the spontaneously broken state in which  $\chi = 0$  is the vanishing Goldstone boson mass. This is an explicit realization of Goldstone's theorem, which is respected by the large  $N$  approximation.

In the following the explicit functional dependence of  $G[\chi]$  and its inverse on the mean field  $\chi$  will be suppressed, and we adopt the simpler notation  $G(x, y)$  or still more briefly  $G$  hereafter.

The important difference of the large  $N$  equations from the purely classical ones is the last term in (2.13) involving  $\hbar G$ . Whereas the spontaneous symmetry breaking solution  $\chi = 0$  can be achieved only when  $\phi = \pm v_0 \equiv \pm\sqrt{2/\lambda\mu}$  classically, in the large  $N$  approximation the two-point function  $G$  contributes at the same order and can even dominate the mean field  $\phi$  in Eqn. (2.13). Since  $G$  itself depends on  $\chi$  this additional term also has the effect that the  $\chi$  field can undergo nonlinear collective plasmon-like oscillations as we shall see explicitly in Section VII. Notice also that there is nothing to prevent  $\chi$  from being negative at some times which allows us to explore the dynamics of the unstable spinodal region of Fig. 3. The spinodal at a given temperature is the region where the second derivative of the potential becomes negative. In the large  $N$  approximation, this corresponds to  $\chi < 0$ .

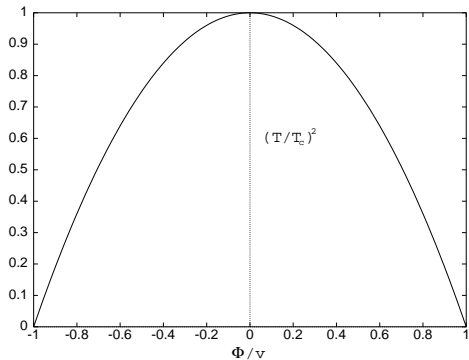


FIG. 3. The spinodal value of  $\phi$ ,  $\phi_T$  is the value of  $\phi$  where  $\chi$  first becomes negative. It satisfies the equation  $(\phi_T/v)^2 = 1 - (T/T_c)^2$  shown above (see Eqn. (4.7) below).

In this paper we shall be concerned only with spatially homogeneous mean fields  $\phi = \phi(t)$  and  $\chi = \chi(t)$ . It is not difficult to treat spatially inhomogeneous mean fields by the same methods, but as the homogeneous case is simpler and already contains much of the essential physics,

we restrict ourselves to that case in this paper. When  $\phi$  and  $\chi$  are functions only of  $t$ , then the two-point Green's function  $G$  is a function only of the spatial difference  $\mathbf{x} - \mathbf{x}'$  and it is useful to introduce the Fourier transform of the corresponding Wightman function  $G_>$  (or  $G_<$ ),

$$G_>(t, \mathbf{x}; t', \mathbf{x}') = -G_<^*(t, \mathbf{x}; t', \mathbf{x}') \\ = \int [d\mathbf{k}] e^{i\mathbf{k}\cdot(\mathbf{x}-\mathbf{x}')} G_>(t, t'; \mathbf{k}) \quad (2.18)$$

with

$$[d\mathbf{k}] \equiv \frac{d^d\mathbf{k}}{(2\pi)^d}. \quad (2.19)$$

In fact,  $G_>$  is a function only of  $k \equiv |\mathbf{k}|$  by rotational symmetry of the spatially homogeneous state. The Wightman functions are solutions of the source-free wave equation  $G^{-1} \circ G_> = G^{-1} \circ G_< = 0$ . In terms of complex mode functions  $f_k(t)$  obeying

$$\left[ \frac{d^2}{dt^2} + k^2 + \chi(t) \right] f_k(t) = 0, \quad (2.20)$$

it is convenient to express the Wightman functions as

$$G_>(t, t'; k) = i f_k(t) f_k^*(t') (N(k) + 1) + i f_k^*(t) f_k(t') N(k), \quad (2.21)$$

where  $N(k)$  (not to be confused with the  $N$  of large  $N$ ) is an arbitrary time-independent function of  $k$ . It carries the interpretation of particle number density in the general spatially homogeneous initial state in the basis specified by the mode functions  $f_k$ , and is arbitrary except for the requirement of being finitely integrable with respect to the integration measure (2.19).

Explicitly, if the original quantum field  $\Phi$  is expanded about its mean value in terms of the quantum modes  $f_k$  and the corresponding plane wave creation and destruction operators  $a_{\mathbf{k}}^\dagger$  and  $a_{\mathbf{k}}$ ,

$$\Phi(t, \mathbf{x}) = \langle \Phi \rangle + \delta\Phi(t, \mathbf{x}) \\ = \phi(t) + L^{-\frac{d}{2}} \sum_{\mathbf{k}} \left( e^{i\mathbf{k}\cdot\mathbf{x}} f_k(t) a_{\mathbf{k}} + e^{-i\mathbf{k}\cdot\mathbf{x}} f_k^*(t) a_{\mathbf{k}}^\dagger \right) \quad (2.22)$$

in a cubical box of finite length  $L$ , then

$$N(k = |\mathbf{k}|) = \langle a_{\mathbf{k}}^\dagger a_{\mathbf{k}} \rangle \quad (2.23)$$

is just the expectation value of the particle number density in this basis. It is also a function only of  $k$  by isotropy of the spatially homogeneous state. The Wightman functions are given then by the usual expressions,

$$\hbar G_>(t, \mathbf{x}; t', \mathbf{x}') = i \langle \delta\Phi(t, \mathbf{x}) \delta\Phi(t', \mathbf{x}') \rangle, \\ \hbar G_<(t, \mathbf{x}; t', \mathbf{x}') = i \langle \delta\Phi(t', \mathbf{x}') \delta\Phi(t, \mathbf{x}) \rangle, \quad (2.24)$$

and the condition  $G_{>} = -G_{<}^*$  follows immediately from the hermiticity of the underlying quantum field  $\delta\Phi$  in (2.22). The commutation relation

$$[a_{\mathbf{k}}, a_{\mathbf{k}'}^\dagger] = \delta_{\mathbf{k}, \mathbf{k}'} \quad (2.25)$$

implies that the complex mode functions should be chosen to satisfy the Wronskian condition,

$$f_k \frac{df_k^*}{dt} - f_k^* \frac{df_k}{dt} = i\hbar, \quad (2.26)$$

in order for the quantum field operator  $\Phi$  to obey the usual canonical commutation relation,

$$\langle [\Phi(t, \mathbf{x}), \frac{\partial \Phi}{\partial t}(t, \mathbf{x}')] \rangle = i\hbar \delta^d(\mathbf{x} - \mathbf{x}'). \quad (2.27)$$

The normalization of the time-independent Wronskian condition (2.26) is the only place where the constant  $\hbar$  enters the mean field equations, which otherwise are quite classical in their time evolution dynamics.

We have not written the *a priori* possible bilinear terms  $f_k f_k$  or  $f_k^* f_k^*$  in (2.21), since they can always be absorbed into a redefinition of  $f_k$  and  $N(k)$  under the transformation,

$$f_k \rightarrow \cosh \gamma_k e^{i\theta_k + i\psi_k} f_k + \sinh \gamma_k e^{i\theta_k - i\psi_k} f_k^* \quad (2.28)$$

without affecting the mode equation (2.20) or Wronskian condition (2.26). This is equivalent to making a Bogoliubov transformation which sets to zero the expectation values of the pair densities  $\langle a_{\mathbf{k}} a_{\mathbf{k}} \rangle = \langle a_{\mathbf{k}}^\dagger a_{\mathbf{k}}^\dagger \rangle = 0$ . Hence there is a natural  $SU(1, 1)$  Heisenberg group structure (for each  $\mathbf{k}$ ) inherent in the leading order large  $N$  equations.

In the gap equation (2.13) the coincidence limit of the Green's function  $G(x, x)$  appears. The coincidence limit of either  $G_{>}, G_{<}$  or the Feynman propagator  $G$  are all identical, so we obtain from Eqns. (2.21) and (2.18) the coincidence limit of any of the Green's functions in the form of an integral over  $\mathbf{k}$  of the Fourier mode functions,

$$\begin{aligned} \hbar G_{>}(t, \mathbf{x}; t, \mathbf{x}) &= \hbar G_{<}(t, \mathbf{x}; t, \mathbf{x}) \\ &= i \int [d\mathbf{k}] |f_k(t)|^2 (2N(k) + 1). \end{aligned} \quad (2.29)$$

Since the mode functions obeying (2.20) and (2.26) behave as

$$f_k(t) \rightarrow \sqrt{\frac{\hbar}{2\omega_k(t)}} \exp\left(-i \int^t dt' \omega_k(t')\right) \quad (2.30)$$

for large  $k$ , where

$$\omega_k(t) \equiv (k^2 + \chi(t))^{\frac{1}{2}}, \quad (2.31)$$

the integral in (2.29) is quadratically divergent in  $d = 3$  spatial dimensions. Introducing an explicit momentum

cut-off  $\Lambda$  and performing the angular  $\mathbf{k}$  integrations, the gap equation (2.13) may be rewritten in the form,

$$\chi(t) = -\mu_\Lambda^2 + \frac{\lambda_\Lambda}{2} \phi^2(t) + \frac{\lambda_\Lambda}{4\pi^2} \int_0^\Lambda k^2 dk |f_k(t)|^2 \sigma_k \quad (2.32)$$

for  $d = 3$ , where we have defined the notation,

$$\sigma_k \equiv 2N(k) + 1. \quad (2.33)$$

The fact that the bare parameters  $\mu_\Lambda$  and  $\lambda_\Lambda$  must depend on the cut-off in order to render the equations independent of  $\Lambda$  in the end has been exhibited explicitly as well. The quadratic divergence in  $d = 3$  is the divergence of the one-loop self energy diagram in Fig. 1 and is absorbed into the bare mass parameter  $\mu_\Lambda$ . One convenient way to effect this mass renormalization is to evaluate (2.32) in the time-independent spontaneously broken vacuum,  $\chi = 0, \phi = v$ , thereby absorbing the quadratic divergence into the relation between the bare and physical expectation value of the field. In this way we eliminate  $\mu_\Lambda^2$  and obtain

$$\begin{aligned} \chi(t) &= \frac{\lambda_\Lambda}{2} (\phi^2(t) - v^2) \\ &\quad + \frac{\lambda_\Lambda}{4\pi^2} \int_0^\Lambda k^2 dk \left\{ |f_k(t)|^2 \sigma_k - \frac{\hbar}{2k} \right\}, \end{aligned} \quad (2.34)$$

which is free of quadratic divergences.

The remaining logarithmic divergence in the mode integral of (2.34) is removed by the logarithmic coupling constant renormalization in the usual way, *i.e.*

$$\lambda_\Lambda = Z_\lambda^{-1}(\Lambda, m) \lambda_R(m^2) \quad (2.35)$$

with

$$\begin{aligned} Z_\lambda(\Lambda, m) &= 1 - \frac{\hbar}{32\pi^2} \lambda_R(m^2) \ln\left(\frac{\Lambda^2}{m^2}\right) \\ &= \left[ 1 + \frac{\hbar}{32\pi^2} \lambda_\Lambda \ln\left(\frac{\Lambda^2}{m^2}\right) \right]^{-1} \end{aligned} \quad (2.36)$$

and  $\lambda_R(m^2)$  the renormalized  $\Phi^4$  coupling defined at some finite mass scale  $m^2$ . By dividing both sides of (2.34) by  $\lambda_\Lambda$  and using Eqns. (2.35) and (2.36), it is straightforward to verify from the large  $k$  behavior of the integrand that the logarithmic dependence on  $\Lambda$  of the integral in (2.34) is cancelled by the logarithm in (2.36). Thus, the resulting equation for  $\chi(t)$  is independent of  $\Lambda$  for  $\Lambda$  large, and  $\chi$  is in fact a renormalization group invariant physical mass squared of the theory. The condition that  $Z_\lambda > 0$  prevents us from taking the cut-off strictly to infinity with  $\lambda_R > 0$  fixed, for otherwise  $Z_\lambda$  from (2.36) would eventually become negative and the theory would become unstable. This is just a reflection of the Landau ghost instability of scalar  $\Phi^4$  field theory, and means that the theory can be sensible and non-trivial

only as an effective field theory equipped with a large but finite cut-off,  $\Lambda$ . This presents no problem in practice as long as  $\Lambda$  is large enough that the physical time evolution, plasma oscillations, damping, *etc.* occur on time scales much greater than  $\Lambda^{-1}$ . In that case, the evolution is numerically quite insensitive to the value of  $\Lambda$  over a very wide range, provided  $\lambda_R$  is not too large [1].

There is no wave function or  $\phi$  renormalization at lowest order in large  $N$  so no further renormalization is required in  $d = 3$  to this order, and Eqns. (2.15), (2.20), and (2.34) together with the constraint on the initial data (2.26) specify a well-defined closed system of evolution equations for the mean fields  $\phi$  and  $\chi$  in interaction with the fluctuations  $f_k$ . Let us emphasize again that these equations differ from the purely classical tree level approximation or the simple one-loop approximation in that the last term of (2.32) or (2.34) couples the fluctuations self-consistently and nonlinearly back on the time-dependent mass gap function  $\chi(t)$ , corresponding to the full sum of daisy and superdaisy diagrams in Fig. 2.

In  $d = 1$  space dimensions the integral in (2.13) is only logarithmically ultraviolet divergent and (2.34) is already well-defined and finite, without any  $\lambda$  renormalization. However, in lower spatial dimensions the small  $k$  or *infrared* behavior of the integral becomes more delicate, and must be treated carefully.

### III. THE EFFECTIVE HAMILTONIAN AND DENSITY MATRIX

The presentation of the large  $N$  equations of motion of the previous section was based on the functional method, in which the extremization of the effective action  $\mathcal{S}_{eff}$  in (2.15) and (2.16) takes the place of the usual Euler-Lagrange variational principle of classical mechanics. The equations so obtained are for the mean values of the field operators and their two-point Green's functions which describe fluctuations about the mean fields. This immediately raises a question: Is there a corresponding Hamilton form of the variational principle for an effective large  $N$  Hamiltonian involving both the mean fields and their fluctuations? In addition one would like to know: To what distribution of field amplitudes in the Schrödinger wave function (or density matrix) do the large  $N$  equations for the one and two-point functions correspond? It is to these questions that we turn in this section. Answering them will lead directly to the true effective potential of nonequilibrium large  $N$  mean field theory.

Let us begin by consideration of the case of  $d = 0$  spatial dimensions, *i.e.* quantum mechanics. The generalization to higher  $d$  will turn out to be straightforward. For  $d = 0$  the Lagrangian  $L_{cl}$  or  $\tilde{L}_{cl}$  of (2.1) or (2.3) is that of an  $N$  component anharmonic oscillator. If  $N = 1$  it reduces to the usual anharmonic double well oscillator. In the  $d = 0$  case there is no  $\mathbf{k}$  index to be integrated and the equations derived in the last section become simply

$$\left(\frac{d^2}{dt^2} + \chi(t)\right)\phi(t) = 0, \\ \chi(t) = \frac{\lambda}{2}(\phi^2(t) + \xi^2(t) - v_0^2), \quad (d = 0) \quad (3.1)$$

where we have introduced the notation,

$$\xi^2(t) \equiv \sigma |f(t)|^2 \equiv (2N + 1) |f(t)|^2 \quad (3.2)$$

in terms of the expectation of the number operator,  $N = \langle a^\dagger a \rangle$ . We recognize that

$$\xi^2(t) = \langle \Phi(t)\Phi(t) \rangle - \phi^2(t) = \langle (\Phi(t) - \phi(t))^2 \rangle \quad (3.3)$$

is just the quadratic variance of the quantum variable  $\Phi(t)$  from its mean value  $\phi(t)$ . By differentiating this relation and defining  $\eta \equiv \dot{\xi}$  we find

$$2\xi(t)\eta(t) = \langle (\dot{\Phi}(t)\Phi(t) + \Phi(t)\dot{\Phi}(t) - 2\phi(t)\dot{\phi}(t)) \rangle \\ = 2\sigma \text{Re}(\dot{f}f^*). \quad (3.4)$$

The advantage of defining these quantities will become apparent from the role they play in the physical interpretation of the equations of motion (3.1) in the Schrödinger picture. Indeed, by differentiating (3.4) again and using both the equation of motion (2.20) (with  $k = 0$  in  $d = 0$  spatial dimensions) and the Wronskian condition (2.26) for  $f(t)$ , we find

$$\dot{\eta} = \ddot{\xi} = -\chi\xi - \frac{\dot{\xi}^2}{\xi} + \frac{\sigma|\dot{f}|^2}{\xi} = -\chi\xi + \frac{\hbar^2\sigma^2}{4\xi^3} \quad (3.5)$$

in the new notation. This equation of motion together with (3.1) are just Hamilton's equations,

$$\dot{p} = -\frac{\partial H_{eff}}{\partial \phi}, \\ \dot{\eta} = -\frac{\partial H_{eff}}{\partial \xi} \quad (3.6)$$

for the effective *two*-dimensional classical Hamiltonian,

$$H_{eff}(p, \phi; \eta, \xi; \sigma) = \frac{1}{2}(p^2 + \eta^2) \\ + \frac{\lambda}{8}(\phi^2 + \xi^2 - v_0^2)^2 + \frac{\hbar^2\sigma^2}{8\xi^2} \quad (3.7)$$

with

$$p \equiv \dot{\phi} = \frac{\partial H_{eff}}{\partial p}, \\ \eta \equiv \dot{\xi} = \frac{\partial H_{eff}}{\partial \eta} \quad (3.8)$$

the canonical momenta conjugate to the two generalized coordinates  $\phi$  and  $\xi$ . A different but equivalent set of canonical variables was discussed in Ref. [7].

Hence by the simple change of notation in (3.2) and (3.4) we have recognized that the large  $N$  equations for

the quantum anharmonic oscillator with classical potential

$$V_{cl}(\Phi) = \frac{\lambda}{8N} \left( \sum_{i=1}^N \Phi_i \Phi_i - v_0^2 \right)^2, \quad (3.9)$$

derived by the effective action technique of the last section are precisely equivalent to Hamilton's equations for the effective Hamiltonian (3.7). This answers the first question we posed at the beginning of this section in the affirmative, at least for the case of  $d = 0$ .

An immediate corollary of the Hamiltonian structure in the extended phase space  $(p, \phi; \eta, \xi)$  is that the large  $N$  evolution equations are energy conserving with  $H_{eff}$  the value of the conserved energy. It is also interesting to note that  $\hbar\sigma$  is a constant of the motion which enters the effective potential

$$U_{eff}(\phi, \xi; \sigma) = \frac{\lambda}{8} (\phi^2 + \xi^2 - v_0^2)^2 + \frac{\hbar^2 \sigma^2}{8\xi^2} \quad (3.10)$$

together as a single ‘‘centrifugal barrier’’ term, whose effect is to repel the variance  $\xi$  away from zero. The physical and mathematical analogy to an angular momentum barrier is made even stronger by the fact that the three symmetric bilinears  $aa$ ,  $a^\dagger a^\dagger$  and  $aa^\dagger + a^\dagger a$  generate the Lie algebra of  $su(1, 1)$  or  $so(2, 1)$  which is the non-compact version of the ordinary angular momentum algebra,  $su(2)$  or  $so(3)$ , and moreover, the Casimir invariant of this rank one Lie algebra is exactly  $\hbar^2 \sigma^2 / 4$ , in the standard normalization. The corresponding Lie group is just the three parameter group of homogeneous linear Bogoliubov transformations (2.28).

To answer the second question posed at the beginning of this section let us recall that both the time-dependent Hartree (TDH) and large  $N$  equations have been studied in the Schrödinger representation, and they are known to correspond to a Gaussian trial wave function ansatz [8]. Indeed, it is straightforward to verify that the Gaussian ansatz for the normalized pure state Schrödinger wave function,

$$\begin{aligned} \Psi(x; t) &\equiv \langle x | \Psi(t) \rangle \\ &= (2\pi\xi^2(t))^{-\frac{1}{4}} \exp \left\{ i \frac{p(t)x}{\hbar} \right. \\ &\quad \left. - \left( \frac{1}{4\xi^2(t)} + i \frac{\eta(t)}{2\hbar\xi(t)} \right) (x - \phi(t))^2 \right\} \end{aligned} \quad (3.11)$$

obeys the expectation value of the Schrödinger equation,

$$\begin{aligned} \langle \Psi(t) | \left\{ -\frac{\hbar^2}{2} \sum_{i=1}^N \frac{\partial^2}{\partial \Phi_i \partial \Phi_i} + V(\Phi) \right\} | \Psi(t) \rangle \\ = i\hbar \langle \Psi(t) | \frac{\partial}{\partial t} | \Psi(t) \rangle \end{aligned} \quad (3.12)$$

in the coordinate representation where, with  $\mathbf{P}$  as the canonical momentum,

$$\begin{aligned} \langle \Psi(t) | \mathcal{O}(\Phi, \mathbf{P}) | \Psi(t) \rangle \\ = \int_{-\infty}^{\infty} dx \Psi^*(x; t) \mathcal{O} \left( x, -i\hbar \frac{\partial}{\partial x} \right) \Psi(x; t), \end{aligned} \quad (3.13)$$

provided the large  $N$  limit is taken and the equations of motion (3.1) and (3.5) are satisfied for  $\sigma = 1$ . Thus, the Gaussian ansatz (3.11) is a special case of the general large  $N$  equations of motion, where  $\xi$  and  $\eta$  are related to the real and imaginary parts respectively of the Gaussian covariance.

In earlier work [9] it had been recognized that the Gaussian ansatz for the Schrödinger wave function(al) imposed one constraint on the *ab initio* three independent symmetrized variances,

$$\begin{aligned} \langle \Psi(t) | (\Phi - \phi)^2 | \Psi(t) \rangle &= \xi^2, \\ \langle \Psi(t) | (\mathbf{P}\Phi + \Phi\mathbf{P} - 2\phi p) | \Psi(t) \rangle &= 2\xi\eta, \\ \langle \Psi(t) | (\mathbf{P} - p)^2 | \Psi(t) \rangle &= \eta^2 + \frac{\hbar^2}{4\xi^2} \text{ (pure state),} \end{aligned} \quad (3.14)$$

expressing all three in terms of only the two variables  $\xi$  and  $\eta$ , in the present notation. The one anti-symmetrized variance is fixed by the commutation relation,  $[\Phi, \mathbf{P}] = i\hbar$ . To what does the restriction to  $\sigma = 1$  correspond and how can it be relaxed? The answer to this question is suggested by the form of (3.14), and definition of  $\sigma$  in (2.33) or (3.2), which shows that  $\sigma = 1$  corresponds to zero expectation of the number operator  $a^\dagger a$ , *i.e.* to the pure state vacuum annihilated by  $a$ . However, the mean field equations of the Section II allow for the more general possibility that this expectation value may take on any constant value  $N$ . For example, we might consider the finite temperature Bose-Einstein distribution,

$$\begin{aligned} N_T &= \left[ \exp \left( \frac{\hbar\omega_0}{kT} \right) - 1 \right]^{-1}, \\ \sigma_T &= 1 + 2N_T = \coth \left( \frac{\hbar\omega_0}{2T} \right) > 1 \end{aligned} \quad (3.15)$$

for some  $\omega_0$  and temperature  $T$ . Since such a thermal state corresponds not to a pure state Schrödinger wave function, but rather to a *mixed* state density matrix, it is not surprising that a pure state Gaussian wave function ansatz cannot describe this case. However, the general structure of the mean field equations involves only the one and two-point functions of the quantum variable, so we should expect them to correspond to a Gaussian ansatz but for a *mixed*-state density matrix instead of a pure state wave function. The most general form for this mixed-state normalized Gaussian density matrix  $\rho$  is

$$\begin{aligned} \langle x' | \rho(p, \phi; \eta, \xi; \sigma) | x \rangle &= (2\pi\xi^2)^{-\frac{1}{2}} \exp \left\{ i \frac{p}{\hbar} (x' - x) \right. \\ &\quad \left. - \frac{\sigma^2 + 1}{8\xi^2} [(x' - \phi)^2 + (x - \phi)^2] \right. \\ &\quad \left. + i \frac{\eta}{2\hbar\xi} [(x' - \phi)^2 - (x - \phi)^2] + \frac{\sigma^2 - 1}{4\xi^2} (x' - \phi)(x - \phi) \right\}, \end{aligned} \quad (3.16)$$

in the coordinate representation. In the special case that  $\sigma = 1$  the last (mixed) term in the exponent vanishes and  $\rho$  reduces to the pure state product,

$$\rho(t) \Big|_{\sigma=1} = |\Psi(t)\rangle\langle\Psi(t)|, \quad (3.17)$$

with  $|\Psi(t)\rangle$  given by (3.11). For  $\sigma > 1$  the general Gaussian  $\rho$  does not decompose into a product, and

$$\begin{aligned} \text{Tr } \rho^2(t) &\equiv \int_{-\infty}^{\infty} dx \int_{-\infty}^{\infty} dx' \langle x|\rho(t)|x'\rangle\langle x'|\rho(t)|x\rangle \\ &= \sigma^{-1} < 1 \end{aligned} \quad (3.18)$$

which is characteristic of a mixed state density matrix.

That (3.16) is indeed the correct generalization of the pure state Gaussian wave function (3.11) is easily verified by checking that  $\rho(t)$  satisfies the expectation value of the quantum Liouville equation,

$$\text{Tr} \left( i\hbar \frac{\partial}{\partial t} \rho \right) = \text{Tr} [\mathbf{H}, \rho], \quad (3.19)$$

provided the large  $N$  limit as before is taken and the equations of motion (3.1) and (3.5) are satisfied for *arbitrary*  $\sigma$ . Taking the large  $N$  limit is equivalent here to the replacement of the full anharmonic Hamiltonian by a time-dependent harmonic oscillator Hamiltonian,

$$\mathbf{H} \rightarrow \mathbf{H}_{osc} = \frac{1}{2} (\mathbf{P}^2 + \omega^2(t) \mathbf{\Phi}^2) \quad (3.20)$$

where

$$\omega^2(t) = \left\langle \frac{\partial^2 V}{\partial \Phi_i \partial \Phi_j} \right\rangle \Big|_{i=j} \rightarrow \frac{\lambda}{2} (\phi^2(t) + \xi^2(t) - v_0^2) = \chi(t) \quad (3.21)$$

is the self-consistently determined frequency of the oscillator in the large  $N$  limit. With this replacement it is straightforward to verify that the Gaussian form is preserved by the time evolution under  $\mathbf{H}_{osc}$  [10] [11] [12],

$$i\hbar \frac{\partial}{\partial t} \rho = [\mathbf{H}_{osc}, \rho]. \quad (3.22)$$

In fact, substitution of the Gaussian form (3.16) into this Liouville equation and equating coefficients of  $x$ ,  $x'$ ,  $x^2$ ,  $x'^2$  and  $xx'$  gives five evolution equations for the five parameters specifying the Gaussian which are none other than the Eqns. (3.1) and (3.5) together with  $\dot{\sigma} = 0$ .

The effective classical Hamiltonian for the large  $N$  equations, (3.7) is just the expectation value of the quantum Hamiltonian in this general mixed state Gaussian density matrix, *i.e.*

$$H_{eff}(\phi, p; \xi, \eta; \sigma) = \text{Tr} (\rho \mathbf{H}) = \text{Tr} (\rho \mathbf{H}_{osc}) = \varepsilon L^d, \quad (3.23)$$

in the large  $N$  limit where  $\varepsilon$  is the energy density defined in (A2). The three symmetrized variances are indeed now all independent with

$$\begin{aligned} \text{Tr} (\rho (\mathbf{\Phi} - \phi)^2) &= \xi^2, \\ \text{Tr} (\rho (\mathbf{P}\mathbf{\Phi} + \mathbf{\Phi}\mathbf{P} - 2\phi p)) &= 2\xi\eta, \\ \text{Tr} (\rho (\mathbf{P} - p)^2) &= \eta^2 + \frac{\hbar^2 \sigma^2}{4\xi^2} \end{aligned} \quad (3.24)$$

replacing (3.14) of the pure state case. The mean values,

$$\phi = \langle \mathbf{\Phi} \rangle = \text{Tr} (\mathbf{\Phi} \rho); \quad \text{and} \quad p = \langle \mathbf{P} \rangle = \text{Tr} (\mathbf{P} \rho) \quad (3.25)$$

remain valid for both the pure and mixed state cases.

The physical interpretation of the five parameters of the general large  $N$  equations ( $p, \phi, \eta, \xi; \sigma$ ) in terms of the general time-dependent mixed-state Gaussian density matrix of the Schrödinger picture is now explicit in  $d = 0$  quantum mechanics. Since  $\sigma$  is the constant parameter which determines the degree of mixing and  $\hbar$  and  $\sigma$  appear only in the combination  $\hbar\sigma$  it is clear that the large  $N$  equations allow for a smooth interpolation between the quantum pure state case in which  $\hbar\sigma = \hbar$  to the high temperature or classical limit where

$$\hbar\sigma_T \rightarrow \frac{2T}{\omega_0} \quad \text{as} \quad T \rightarrow \infty \quad \text{or} \quad \hbar \rightarrow 0, \quad (3.26)$$

in which  $\hbar$  drops out entirely. Thus, quantum and classical thermal fluctuations are treated on the same footing in the large  $N$  limit, with the value of the constant parameter  $\hbar\sigma$  determining whether the fluctuations described by  $\xi$  and  $\eta$  are to be regarded as predominantly quantal or thermal, or intermediate between the two. Moreover, we see that large  $N$  Gaussian dynamics is really classical dynamics of a Gaussian distribution function, except that  $\hbar\sigma$  which measures the second moment of the classical distribution cannot be taken to zero as it could be classically, but instead is bounded from below by  $\hbar$ . This is made explicit by the form of the Wigner function corresponding to the density matrix (3.16), *viz.*

$$\begin{aligned} f_W(x, p_x) &\equiv \frac{1}{2\pi\hbar} \int_{-\infty}^{\infty} dy e^{-ip_x y/\hbar} \langle x + \frac{y}{2} | \rho | x - \frac{y}{2} \rangle \\ &= \frac{1}{\pi\hbar\sigma} \exp \left\{ -\frac{(x - \phi)^2}{2\xi^2} - \frac{2\xi^2}{\hbar^2\sigma^2} \left[ p_x - \phi - \frac{\eta}{\xi}(x - \phi) \right]^2 \right\}. \end{aligned} \quad (3.27)$$

Before leaving our  $d = 0$  example it is instructive to examine the static solutions of the effective Hamiltonian, *viz.* the simultaneous vanishing of

$$\begin{aligned} \dot{p} &= -\frac{\partial H_{eff}}{\partial \phi} = -\frac{\lambda}{2} (\phi^2 + \xi^2 - v_0^2) \phi = \chi \phi = 0, \quad \text{and} \\ \dot{\eta} &= -\frac{\partial H_{eff}}{\partial \xi} = -\chi \xi + \frac{\hbar^2 \sigma^2}{4\xi^3} = 0. \end{aligned} \quad (3.28)$$

If we look for a spontaneously broken solution  $\phi \neq 0$ , then  $\chi$  must vanish from the first of these conditions. But then we cannot satisfy the second condition for finite  $\hbar\sigma$  and  $\xi$ . This is just a rederivation of the fact that there can be no spontaneous symmetry breaking in  $d = 0$  quantum mechanics (or in fact for any  $d \leq 1$ ). We are forced instead to the symmetry restored situation for which  $\phi = 0$  and  $\chi = \chi_0 > 0$  is determined from the real positive root of the cubic equation

$$\chi_0 = \frac{\lambda}{2}(\xi_0^2 - v_0^2) = \frac{\hbar^2\sigma^2}{4\xi_0^4} \quad (3.29)$$

for  $\xi_0^2(\sigma)$ . The Gaussian density matrix centered at  $\phi = 0$  with variance  $\xi_0^2(\sigma)$  is the solution of the time-independent Liouville equation for the anharmonic double well oscillator with a trial variational density matrix of the form (3.16). In the limit that the height of the energy barrier between the two wells,  $E_b = \lambda v_0^4/8$  is much greater than the fluctuation energy in either well,  $E_f = \hbar\sigma\sqrt{\lambda}v_0/2$ , the width of the Gaussian  $\xi_0^2 \rightarrow v_0^2$ , and its energy  $E_0 \rightarrow \hbar^2\sigma^2/8v_0^2 = E_f^2/16E_b \ll E_f$ , corresponding to a probability density spread over the entire region  $(-v_0, v_0)$  in all  $N$  components of  $\Phi_i$ .

The entire development of the Hamiltonian equations and Gaussian density matrix is quite easy to generalize to any number of spatial dimensions  $d$ , at least for the case of spatially homogeneous mean fields. Since in Fourier space the mode equations are just replicated at every spatial momentum  $\mathbf{k}$  we have simply to introduce the subscript  $\mathbf{k}$  on all of the relevant definitions in this section. For example, the density matrix for  $d > 0$  can be written as a product of Gaussians in Fourier space, *viz.*

$$\begin{aligned} \langle \{\varphi_{\mathbf{k}}\}' | \rho | \{\varphi_{\mathbf{k}}\} \rangle &= \prod_{\mathbf{k}} \langle \{\varphi_{\mathbf{k}}\}' | \rho(p_{\mathbf{k}}, \phi_{\mathbf{k}}; \eta_{\mathbf{k}}, \xi_{\mathbf{k}}; \sigma_{\mathbf{k}}) | \{\varphi_{\mathbf{k}}\} \rangle \\ &= \prod_{\mathbf{k}} (2\pi\xi_{\mathbf{k}}^2)^{-\frac{1}{2}} \exp \left\{ i \frac{p_{\mathbf{k}}}{\hbar} (\varphi_{\mathbf{k}}' - \varphi_{\mathbf{k}}) \right. \\ &\quad - \frac{\sigma_{\mathbf{k}}^2 + 1}{8\xi_{\mathbf{k}}^2} [(\varphi_{\mathbf{k}}' - \phi_{\mathbf{k}})^2 + (\varphi_{\mathbf{k}} - \phi_{\mathbf{k}})^2] \\ &\quad + i \frac{\eta_{\mathbf{k}}}{2\hbar\xi_{\mathbf{k}}} [(\varphi_{\mathbf{k}}' - \phi_{\mathbf{k}})^2 - (\varphi_{\mathbf{k}} - \phi_{\mathbf{k}})^2] \\ &\quad \left. + \frac{\sigma_{\mathbf{k}}^2 - 1}{4\xi_{\mathbf{k}}^2} (\varphi_{\mathbf{k}}' - \phi_{\mathbf{k}})(\varphi_{\mathbf{k}} - \phi_{\mathbf{k}}) \right\}, \quad (3.30) \end{aligned}$$

where  $\varphi_{\mathbf{k}}$  is the generalized coordinate of the field amplitude in Fourier space and  $p_{\mathbf{k}}$  the corresponding canonical momentum. The mean fields and their canonical momenta

$$\phi_{\mathbf{k}} = \delta_{\mathbf{k}0}\phi(t), \quad p_{\mathbf{k}} = \delta_{\mathbf{k}0}p(t) \quad (3.31)$$

all vanish except for  $\mathbf{k} = 0$  in the spatially homogeneous case. The definitions

$$\xi_{\mathbf{k}}^2(t) \equiv \sigma_{\mathbf{k}} |f_{\mathbf{k}}(t)|^2 \equiv (2N(k) + 1) |f_{\mathbf{k}}(t)|^2, \quad \eta_{\mathbf{k}} \equiv \dot{\xi}_{\mathbf{k}} \quad (3.32)$$

and

$$\begin{aligned} \chi(t) &= \frac{\lambda}{2} \left( \phi^2(t) + \int [d\mathbf{k}] \xi_{\mathbf{k}}^2(t) - v_0^2 \right) \\ &= \frac{\lambda}{2} \left[ \phi^2(t) + \int [d\mathbf{k}] \left( \xi_{\mathbf{k}}^2(t) - \frac{\hbar}{2k} \right) - v^2 \right] \quad (3.33) \end{aligned}$$

have been introduced in obvious analogy to the  $d = 0$  case. The effective Hamiltonian density which gives rise to these equations is

$$\frac{H_{eff}}{L^d} = \varepsilon = \frac{1}{2}p^2 + \frac{1}{2\lambda}\chi^2 + \frac{1}{2} \int [d\mathbf{k}] \left( \eta_{\mathbf{k}}^2 + k^2\xi_{\mathbf{k}}^2 + \frac{\hbar^2\sigma_{\mathbf{k}}^2}{8\xi_{\mathbf{k}}^2} \right) \quad (3.34)$$

with  $\chi$  regarded as a dependent variable of  $\phi$  and the  $\xi_{\mathbf{k}}$  through the gap equation (3.33) above. The  $k^2$  term arising from the spatial gradient of the field in  $d > 0$  dimensions is the most significant difference from the  $d = 0$  case considered previously. The Hamiltonian equations of motion

$$\begin{aligned} \dot{\phi} &= p, & \dot{p} &= -\frac{\partial H_{eff}}{\partial \phi} = -\chi\phi, \\ \dot{\xi}_{\mathbf{k}} &= \eta_{\mathbf{k}}, & \dot{\eta}_{\mathbf{k}} &= -\frac{\partial H_{eff}}{\partial \xi_{\mathbf{k}}} = -(k^2 + \chi)\xi_{\mathbf{k}} + \frac{\hbar^2\sigma_{\mathbf{k}}^2}{4\xi_{\mathbf{k}}^3} \end{aligned} \quad (3.35)$$

are completely equivalent to the equations of motion for the mode functions (2.20) and mean fields (2.15) and (2.13) in the spatially homogeneous case in any number of dimensions.

This completes our demonstration that the large  $N$  mean field equations of the previous section are Hamilton's equations with  $H_{eff}$  given explicitly by (3.34) above, and the identification of the time-dependent Gaussian density matrix (3.30) to which the homogeneous mean field equations correspond. The case of spatially inhomogeneous mean fields involves only the straightforward generalization of (3.30) to Gaussian covariances which are off-diagonal in the momentum index  $\mathbf{k}$ , and a corresponding coupling between the different momentum modes in the effective Hamiltonian (3.34). Since we have no need of these expressions in the present work we do not give the explicit formulae here, though they may be easily worked out within the present framework.

#### IV. THE NONEQUILIBRIUM TRUE EFFECTIVE POTENTIAL (TEP)

Having obtained the effective Hamiltonian which describes the evolution of the closed system of mean fields and fluctuations in the large  $N$  limit, it is natural to define the dynamical or true effective potential to be the static part of the effective Hamiltonian density (3.34), *i.e.*

$$\begin{aligned}
U_{eff}(\phi, \{\xi_k\}; \{\sigma_k\}) & \\
&\equiv \frac{1}{2\lambda}\chi^2 + \frac{1}{2} \int [d\mathbf{k}] \left( k^2 \xi_k^2 + \frac{\hbar^2 \sigma_k^2}{8\xi_k^2} \right) \quad (4.1) \\
&= \frac{\chi}{2} \left( \phi^2 - v_0^2 - \frac{\chi}{\lambda} \right) + \frac{1}{2} \int [d\mathbf{k}] \left( (k^2 + \chi) \xi_k^2 + \frac{\hbar^2 \sigma_k^2}{4\xi_k^2} \right).
\end{aligned}$$

This  $U_{eff}$  is the energy density of an initial state with a Gaussian density matrix (3.30) centered around  $\phi$  with instantaneously zero velocities  $p = \eta_k = 0$  in both the mean field and the fluctuation variables. We call  $U_{eff}$  the ‘‘True Effective Potential’’ (TEP) because it determines the true out-of-equilibrium time evolution dynamics of the system according to Hamilton’s Eqns. (3.35). It must be clearly distinguished from the finite temperature free energy effective potential often discussed in the literature. The relationship between the two we would like to discuss next.

The standard method of calculating the free energy at temperature  $T$  is to analytically continue the effective action  $\mathcal{S}_{eff}$  to imaginary time [13] and evaluate the  $\text{Tr} \ln G^{-1}$  term over fluctuations which are periodic in imaginary time with period  $\beta = \hbar/T$ . In this way one finds for the case at hand,

$$\begin{aligned}
&\frac{\chi}{2} \left( \phi^2 - v_0^2 - \frac{\chi}{\lambda} \right) \\
&+ \int [d\mathbf{k}] \left\{ \frac{\hbar\omega_k}{2} + T \ln \left[ 1 - \exp \left( -\frac{\hbar\omega_k}{T} \right) \right] \right\}, \quad (4.2)
\end{aligned}$$

which is a real function of  $\phi$  provided

$$\omega_k^2 = k^2 + \chi \geq 0. \quad (4.3)$$

The infinite zero point energy in  $F$  is handled in the usual way by subtracting the energy of the zero temperature vacuum at  $\chi = 0$ , *i.e.*  $\int [d\mathbf{k}] \hbar k/2$ . With the subtraction of this temperature independent constant and the previous definitions of  $v$  and the logarithmic coupling renormalization by Eqns. (2.35) and (2.36), the thermodynamic free energy becomes finite and is given by [14]:

$$\begin{aligned}
F(\phi, T) &= \frac{\chi_T}{2} \left( \phi^2 - v^2 - \frac{\chi_T}{\lambda} \right) \\
&+ \frac{\hbar}{4\pi^2} \int_0^\infty k^2 dk \left\{ \omega_k - k - \frac{\chi_T}{2k} \right. \\
&\left. + 2T \ln \left[ 1 - \exp \left( -\frac{\hbar\omega_k}{T} \right) \right] \right\}, \quad (4.4)
\end{aligned}$$

with  $\chi_T$  the solution of the finite temperature gap equation,

$$\begin{aligned}
\chi_T(\phi) &= \frac{\lambda}{2} (\phi^2 - v^2) \\
&+ \frac{\hbar\lambda}{8\pi^2} \int_0^\infty k^2 dk \left\{ \frac{1}{\omega_k} \coth \left( \frac{\hbar\omega_k}{2T} \right) - \frac{1}{k} \right\}. \quad (4.5)
\end{aligned}$$

As long as  $\chi_T \geq 0$  the free energy function (4.4) is real and well-defined.

The first derivative of the free energy function is given by

$$\frac{dF}{d\phi} = \chi_T \phi \quad (4.6)$$

upon using the gap equation (4.5). In the spontaneously broken state defined by  $\chi_T = 0$ , we have

$$\begin{aligned}
\phi^2 = \phi_T^2 &= v^2 - \frac{\hbar}{2\pi^2} \int_0^\infty k dk \frac{1}{\exp \left( \frac{\hbar k}{T} \right) - 1} \\
&= v^2 - \frac{T^2}{12\hbar}. \quad (4.7)
\end{aligned}$$

The last relation informs us that the expectation value  $\phi_T$  vanishes at the critical temperature,

$$T_c = 2\sqrt{3\hbar} v. \quad (4.8)$$

At  $T = T_c$ , the second derivative of  $F(\phi, T)$  vanishes at  $\phi = 0$ , and therefore the phase transition is second order in the large  $N$  approximation. We remark that this is *not* the case in the simple one-loop or Hartree approximation where the transition is weakly first order [15]. Since the  $\Phi^4$  field theory lies in the same universality class as spin models which are known to have second order phase transitions, the large  $N$  mean field approximation gets the correct order of the transition, and is another reason why it is to be preferred over the other approximations [16]. Indeed, the correlation length, which is given by the the inverse mass of the radial excitation,

$$\ell(T) = \lambda_R^{-\frac{1}{2}} \phi_T^{-1} \rightarrow \left( \frac{6}{\lambda_R T_c} \right)^{\frac{1}{2}} (T_c - T)^{-\frac{1}{2}} \quad (4.9)$$

diverges as  $T \rightarrow T_c$  with the  $-\frac{1}{2}$  critical exponent of mean field theory.

Actually the second derivative of the free energy function vanishes at its minimum for *any*  $T \leq T_c$ . This follows the fact that the derivative of the gap equation (4.5) evaluated at  $\chi_T = 0$  involves an infrared linear divergence so that

$$\left. \frac{d\chi_T(\phi)}{d\phi} \right|_{\chi_T=0} = 0, \quad (4.10)$$

and

$$\frac{d^2 F}{d\phi^2} = \chi_T + \frac{d\chi_T(\phi)}{d\phi} \phi = 0 \quad (4.11)$$

at  $\chi_T = 0$ . This perhaps surprising feature of the large  $N$  free energy is illustrated in Fig. 4. It is a direct consequence of the massless Goldstone particles present in the spontaneously broken phase. As we shall see in Section VII, it also makes the equilibrium free energy useless for describing the plasma oscillations about the spontaneously broken thermal minimum.

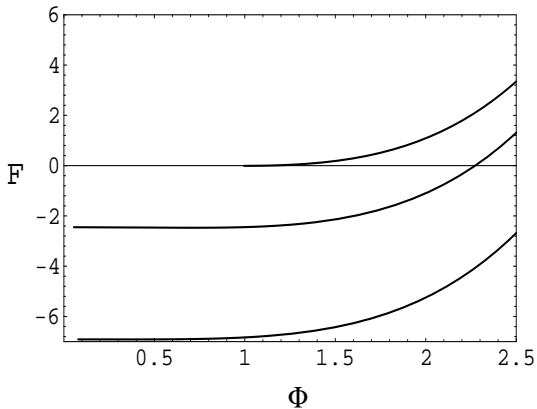


FIG. 4. The Helmholtz Free Energy  $F$  as a function of  $\phi$  for three temperatures  $T = .1, 1, 1.5$  (in descending order from the top) in units of  $T_c$  in the leading order large  $N$  approximation. The curves terminate at the minimum of  $F$  at  $\phi = \phi_T$ ,  $\chi_T = 0$ , given by Eqn. (4.7), which is the boundary of the spinodal region, *i.e.* for  $\phi < \phi_T$  there is no stable equilibrium state. The second derivative of  $F$  at  $\phi = \phi_T$  vanishes, showing in particular that the phase transition at  $T = T_c$  is second order.

For  $T < T_c$  and  $\phi < \phi_T$  the gap equation (4.5) has no positive real solutions. This is the unstable spinodal region of Fig. 3. If  $\chi < 0$  then the frequency  $\omega_k$  becomes imaginary for  $k < |\chi|^{\frac{1}{2}}$ . This means that strictly speaking the thermodynamic free energy  $F$  is not well defined in this region. Despite the fact that no thermal equilibrium uniform state can exist in this spinodal region, what is sometimes done is to *define* the free energy by an analytic continuation from  $\chi > 0$  to  $\chi = -|\chi| < 0$ . By this procedure  $F$  acquires an imaginary part, while its real part is no longer a convex function of  $\phi$  (as general theorems require). This has led to much discussion in the literature [17] [18]. However, we needn't wonder at the meaning of this analytic continuation and imaginary part of  $F$  in the more general nonequilibrium context. The analytic continuation from  $\chi > 0$  to  $\chi = -|\chi| < 0$  simply defines a Gaussian density matrix centered at  $\phi < \phi_T$  with instantaneously zero velocities,  $\dot{\phi} = \eta_k = 0$  and parameters  $\xi_k$  and  $\sigma_k = 2N_T(k) + 1$  determined by the thermal distribution at  $|\chi_T| = -\chi_T$  where the free energy is well defined. The density matrix will certainly evolve away from this unstable configuration and the imaginary part is a measure of the rate at which this evolution will occur initially [2]. However, shortly afterwards the non-linear effects of the evolution described by our general nonequilibrium equations of motion will set in, and this imaginary part can only be at best a simple order of magnitude estimate for the evolution away from the initial state in the weak coupling limit  $\lambda_R \ll 1$ .

The nonconvexity of the real part of the free energy is also related to the same instability [18]. The point is that the construction of the equilibrium free energy by a loop expansion or the large  $N$  expansion tacitly assumes the

existence of a stable configuration as the starting point for the expansion. It is precisely this assumption which breaks down in the unstable spinodal region. A careful definition of the “effective potential”  $F$  as the minimum of the free energy for fixed  $\phi = \langle \Phi \rangle$  independent of space and time leads to a flat constant function between the two minima at  $\pm v$  which is convex in accordance with the general theorems. However this minimization cannot be achieved with a Gaussian density matrix of the form (3.30) and the flat convex form of  $F$  defined in this manner tells us nothing about the dynamical evolution of an initial Gaussian centered at a value of  $\phi$  in the spinodal region. For this reason we propose to drop all attempts to refine the definition of a free energy “effective potential” and focus instead on the potential which actually governs the nonequilibrium dynamics in a given approximation scheme. In the leading order large  $N$  scheme this dynamical potential is the True Effective Potential  $U_{eff}$ .

In contrast to the free energy  $F$ , the TEP  $U_{eff}$  is a function(al) of all of the generalized fluctuation coordinates  $\xi_k$  as well as the mean field  $\phi$ . It also depends on the constant parameters  $\sigma_k$ , which need not be that in the thermal distribution (3.15). Hence it is defined much more generally than  $F$  and is manifestly real and positive. If we wish to consider a function only of the mean field  $\phi$  it is possible to try first minimizing  $U_{eff}$  with respect to the Gaussian parameters  $\xi_k$ :

$$\frac{\partial U_{eff}}{\partial \xi_k} = (k^2 + \chi) \xi_k - \frac{\hbar^2 \sigma_k^2}{4\xi_k^3} = 0 \quad (4.12)$$

which has the real solution,

$$\bar{\xi}_k^2 = \frac{\hbar \sigma_k}{2\omega_k} \quad (4.13)$$

provided again that (4.3) holds.

If we restrict  $U_{eff}$  further by requiring  $\sigma_k$  to be the Bose-Einstein thermal distribution,  $\sigma_{T k} = 1 + 2N_T(k)$  of (3.15) we find

$$\begin{aligned} U(\phi, T) &\equiv U_{eff}(\phi, \{\xi_k\} = \{\bar{\xi}_k\}; \sigma_k = \sigma_{T k}) \\ &= \frac{\chi}{2} \left( \phi^2 - v_0^2 - \frac{\chi}{\lambda} \right) \\ &\quad + \frac{\hbar}{2} \int [d\mathbf{k}] \omega_k (1 + 2N_T(k)). \end{aligned} \quad (4.14)$$

The first term is the classical potential energy density  $V_{cl}$  of the mean field  $\phi$  and the second term is the quantum plus thermal energy of the fluctuations at the extremum (4.13). We recognize the expression (4.14) as the *internal* energy of the Gaussian configuration specified by (4.13) and (3.15), which differs from the Helmholtz free energy  $F$  by the standard thermodynamic relation,

$$F = U - T S, \quad (4.15)$$

with

$$\begin{aligned}
S &= -\text{Tr } \rho_T \ln \rho_T \\
&= \int [d\mathbf{k}] [(N_T(k) + 1) \ln (N_T(k) + 1) - N_T(k) \ln N_T(k)]
\end{aligned}
\tag{4.16}$$

the von Neumann entropy of a Gaussian thermal density matrix  $\rho_T$ .

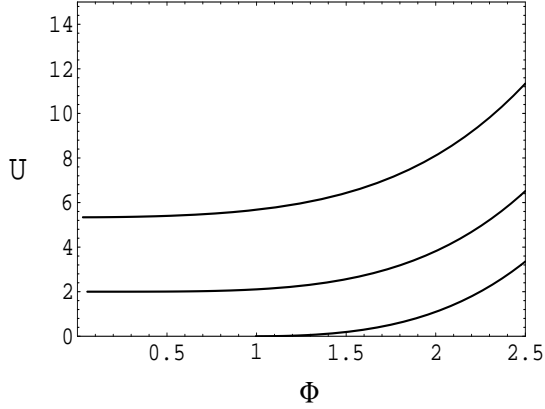


FIG. 5. The True Effective Potential  $U_{eff}$  as a function of  $\phi$  and evaluated in a thermal equilibrium state for the same three temperatures as in the previous figure (note here that the lowest temperature is now the bottom curve). The Gaussian width parameter  $\xi_k$  has been set equal to its minimum value by Eqn. (4.12). Although qualitatively similar to the free energy  $F$  in Fig. 4,  $U_{eff}$  becomes equal to the internal energy  $U$  in thermal equilibrium.

Although  $F$  and  $U$  have qualitatively similar behaviors in the region  $\chi \geq 0$  where they are both defined unambiguously, as shown in Figs. 4 and 5, clearly  $F$  and  $U$  have quite different physical meanings and applicability. The first is the negative of the pressure of the gas of scalar particles against which work must be done in compressing the system at fixed temperature, *i.e.* if the compression is performed while in contact with an external heat reservoir at temperature  $T$ . The second is the energy density of the *closed* system which is conserved if it is allowed to evolve, isolated from all external sources or sinks of energy. The free energy  $F$  can be defined only in thermal equilibrium. The internal energy  $U$  is a special case of the more general true effective potential  $U_{eff}$  which is defined for any Gaussian density matrix, equilibrium or not, and which determines the evolution of the system away from the instantaneous stationary state where  $\dot{\phi} = \dot{\xi}_k = 0$  according to the Hamiltonian equations, (3.35). Moreover, in the spinodal region where  $T < T_c$  and  $\phi < \phi_T$  it is clear that the minimization condition (4.12) cannot be satisfied for real  $\xi_k^2$ , which informs us that the time derivative of the canonical momentum,  $\dot{\eta}_k > 0$  for  $k^2 < |\chi|$ , *i.e.* the configuration is unstable against the fluctuation widths  $\xi_k$  growing in time for these low  $k$ . Note that by the definition (3.32), in terms of the mode function  $f_k$ ,  $\xi_k$  is necessarily real. The phys-

ical interpretation is thus quite straightforward in the more general nonequilibrium framework we have laid out: there simply is no stationary Gaussian density matrix for  $\chi < 0$ , and any such initial configuration will necessarily evolve in time by growth of the small  $k$  Fourier components of the Gaussian parameters  $\xi_k$ . Indeed, this is obvious from the mode equations (2.20) which show that all the long wavelength modes with  $k^2 \leq |\chi|$  will grow exponentially rather than oscillate when  $\chi < 0$  [2]. Notice that the non-existence of a solution to the minimization condition (4.12) implies that the exponentially growing instability lies in the fluctuations  $\xi_k$  for small  $k$ . Only the nonlinear back reaction of this exponential growth of the modes in the time-dependent gap equation (2.13) can eventually bring  $\chi$  to non-negative values and turn off the instability. It is clear that this time-dependent process involves many low  $k$  Fourier components of the field  $\Phi$  and cannot be described adequately by a single function of one variable such as the “effective” potential  $F$ , much less a function of one variable defined only in thermal equilibrium in the spinodal region where no such thermal equilibrium exists.

That the time evolution as determined by  $U_{eff}$  is quite different from what might be inferred from the free energy function  $F$  is illustrated by our numerical solution of the evolution equations, presented in Fig. 6. The oscillation frequency and even the final point of the evolution of  $\phi$  as  $t \rightarrow \infty$  in general bear no simple relation to the minimum  $\phi_T$  of the free energy “effective” potential. This is easily understood from the stationary points of the TEP, for a true stationary state does exist in the spontaneously broken phase if we also require

$$\frac{\partial U_{eff}}{\partial \phi} = \chi \phi = 0
\tag{4.17}$$

since this is satisfied by

$$\chi = 0 ; \quad \text{and} \quad \xi_k^2 = \frac{\hbar \sigma_k}{2k} .
\tag{4.18}$$

Notice that there is such a static solution for *any*  $\phi$  and  $\sigma_k$ . The finite temperature case, (3.15) is only one of infinitely many possibilities for a static solution of the mean field equations. Correspondingly there are also an infinite number of stationary density matrices satisfying  $[\rho, \mathbf{H}_{osc}] = 0$ , one for each choice of  $\sigma_k$ . If  $\sigma_k = 1 + 2N(k)$  is given, then  $\phi$  is determined by the static condition  $\chi = 0$ , *i.e.*

$$\phi^2|_{\chi=0} = v^2 - \hbar \int [d\mathbf{k}] \frac{N(k)}{k} = v^2 - \frac{\hbar}{2\pi^2} \int_0^\infty k dk N(k) .
\tag{4.19}$$

For arbitrary  $N(k)$  the relation (4.19) may be viewed as a kind of sum rule which allows us to distribute any fraction of the  $v^2$  in the coherent vacuum expectation value  $\phi^2$  and the remainder in the integral over particle fluctuation modes. In particular, one may even consider

the case where the mean field  $\phi = 0$  identically, but the theory is still in the spontaneously broken phase since  $\chi$  vanishes and the integral in (4.19) saturates  $v^2$ . This case is a kind of marginal symmetry breaking since any small perturbation of  $\phi$  will take us away from zero mean field.

With the help of the sum rule (4.19) one can easily understand the perhaps initially surprising result, first found numerically in Ref. [19], that the evolution of the  $\phi$  mean field can settle to a value different from, and even much smaller than the thermal equilibrium value  $\phi_T$ . It simply corresponds to the fact that the distribution of particles in the final state is not at all a thermal one. Obviously such a situation cannot be described by the thermodynamic free energy  $F$  since its evaluation by continuation to imaginary time assumes from the outset a thermal distribution of particles. For this reason one could not expect the true evolution according to the mean field equations of motion to bear much relation to what one might infer from an uncritical use of  $F$ , particularly in the region  $\phi < \phi_T$  where no thermodynamic uniform equilibrium state exists and the Helmholtz free energy is not even strictly defined.

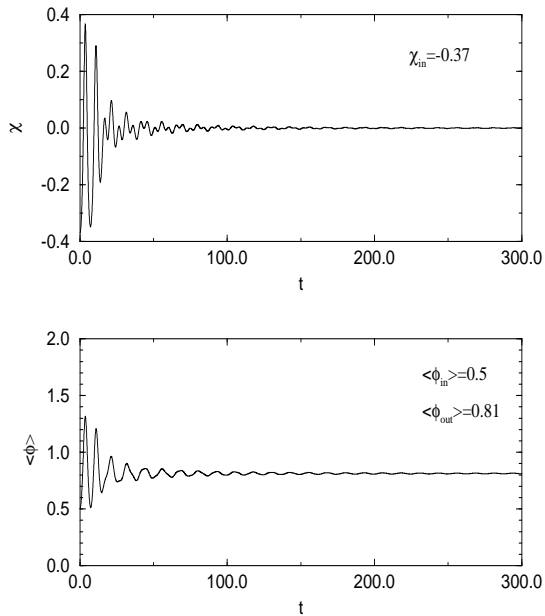


FIG. 6. A typical evolution of the mean field  $\phi$  and the mass squared  $\chi$  in the spontaneously broken phase, starting from an unstable initial state with  $\chi(0) = -0.37 < 0$ . All time and lengths are measured in units of  $v = 1$ . Note that if we use the initial energy density  $\varepsilon = 0.0697$  to infer an effective temperature of massless bosons, then the expected minimum of  $F$  occurs at  $\phi_{out} = 0.98$  which is considerably different than the observed  $\phi_{out} = 0.81$ . The oscillation frequency about  $\phi = \phi_{out}$  also bears no relation to the second derivative of  $F$  which vanishes at its minimum.

The inclusion of collisions in the next order of the expansion in  $1/N$  makes it more likely to bring the dis-

tribution of particles closer to a thermal one. However, since the evolution is unitary, this can happen only in some effective sense. This aspect is closely connected to the notion of dephasing which will be discussed in detail in Section VI.

Finally we point out that the stationary spontaneously broken solution  $\chi = 0$  is disallowed in  $d = 1$  spatial dimension (as it was in  $d = 0$  quantum mechanics), since the integration in the definition of  $\chi$  in (3.33) diverges logarithmically as  $k \rightarrow 0$  which is inconsistent with  $\chi$  vanishing in (4.18). It is this infrared divergence which prevents spontaneous symmetry breaking of the global  $O(N)$  symmetry in one space dimension, consistent with the Mermin-Wagner-Coleman theorem [4]. In two or higher space dimensions there is no such divergence and the spontaneous symmetry breaking static solution (4.18) is allowed.

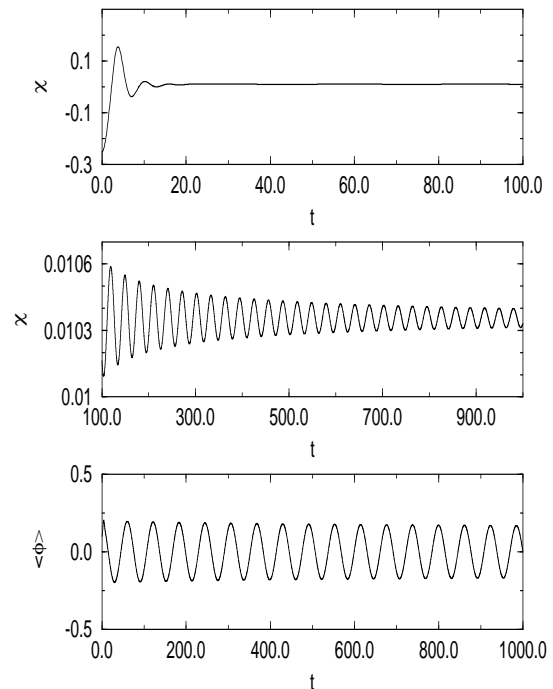


FIG. 7. Evolution of the mean field  $\phi$  and the mass squared  $\chi$  in one space dimension, starting from an unstable initial state. The middle figure shows that  $\chi$  does not go to zero asymptotically, and the oscillations do not damp as effectively as in three dimensions. Both these behaviors are consequences of the Mermin-Wagner-Coleman theorem which prevents spontaneous symmetry breaking in one space dimension.

The consequences of the Mermin-Wagner-Coleman theorem for nonequilibrium dynamics in one dimension are illustrated in Fig. 7 where the numerical evolution of  $\chi$  and  $\phi$  is shown beginning from an unstable initial state with negative  $\chi$ . We see that  $\chi$  does not go to zero at late times (no symmetry breaking) and that both the  $\chi$  and  $\phi$  oscillations damp very slowly as compared to the

behavior in three dimensions.

## V. DEPHASING, DISSIPATION AND DECOHERENCE

Although we have shown by explicit construction of the effective Hamiltonian (3.34) that the large  $N$  mean field equations are completely time reversible, nevertheless one observes in typical evolutions as in Fig. 6 an *effective irreversibility*, in the sense that energy flows from the mean fields  $\phi$  and  $\chi$  to the fluctuating modes  $f_k$  without returning over times of physical interest. It is our purpose in this section to explain this apparent irreversibility in terms of *dephasing*, *i.e.* the dynamical averaging to zero in the sums over  $k$  of the rapidly varying phases of the fluctuations at a given time. To the extent that this phase averaging is exact and the information in the phases cannot be recovered, the time evolution is irreversible. This is the sense in which the fluctuations  $f_k$  act as a “heat bath” or “environment” for the mean field evolution of  $\phi$  and  $\chi$ . Of course, since information is never truly “lost” in a closed Hamiltonian system evolved with arbitrarily high accuracy, the information in the phases can be recovered in principle and we should expect Poincaré recurrences in the mean field evolution after very long times. As the number of modes  $f_k$  (and particularly as the number of relevant infrared modes) approaches infinity, we would expect the recurrence time to go to infinity. In typical evolutions we followed several tens of thousands of modes, and recurrences were never observed in practice. The precise dependence of the recurrence time on the number of modes is an interesting question which may be studied quantitatively within our mean field framework by numerical methods. However, we have not undertaken such a systematic study here, and leave the question of the recurrence time for future research. In any case, we cannot expect the leading order large  $N$  collisionless approximation to continue to be valid for times longer than the collisional relaxation time in the full theory. The study of recurrence times in the leading order approximation may be interesting nevertheless as a model for how such recurrences and rephasing can occur in more realistic situations.

To understand precisely what is meant by dephasing let us return to the Gaussian density matrix of only one degree of freedom (3.16). The coordinate representation is only one of many possible representations of the density matrix. The number basis, defined by the integer eigenvalues of

$$a^\dagger a |n\rangle = n |n\rangle \quad (5.1)$$

defines a time-independent basis associated with the Fock decomposition of the Heisenberg operators (for  $d = 0$ ),

$$\begin{aligned} \Phi(t) &= \phi(t) + af(t) + a^\dagger f^*(t), \\ \dot{\Phi}(t) &= \mathbf{P}(t) = \dot{\phi}(t) + a\dot{f}(t) + a^\dagger \dot{f}^*(t), \end{aligned} \quad (5.2)$$

in terms of its mean value and quantized fluctuations. By using the Wronskian condition (2.26) we may solve these relations for  $a$  and  $a^\dagger$ ,

$$\begin{aligned} (\Phi - \phi)\dot{f}^* - (\mathbf{P} - \dot{\phi})f^* &= i\hbar a, \\ (\Phi - \phi)\dot{f} - (\mathbf{P} - \dot{\phi})f &= -i\hbar a^\dagger. \end{aligned} \quad (5.3)$$

In this time independent basis, the Hamiltonian is given by

$$H = \hbar\omega(t=0) \left( a^\dagger a + \frac{1}{2} \right). \quad (5.4)$$

This transformation is just a (complex) canonical transformation which on the quantum level is implemented by a unitary transformation of bases, with the transformation matrix,  $\langle x|n\rangle$  in Dirac’s notation. To find this transformation matrix explicitly we use the definitions (3.2) and (3.4), the equation of motion (3.5), and the Wronskian condition again to secure

$$\begin{aligned} \hbar^2\sigma \left( a^\dagger a + \frac{1}{2} \right) &= (\Phi - \phi)^2 \left( \frac{\eta^2}{\sigma} + \frac{\hbar^2\sigma^2}{\xi^2} \right) + \xi^2(\mathbf{P} - p)^2 \\ &\quad - \xi\eta((\Phi - \phi)(\mathbf{P} - p) + (\mathbf{P} - p)(\Phi - \phi)) \end{aligned}$$

in terms of  $\xi$ ,  $\eta$ , and  $\sigma$ . Then by acting with this operator identity on the matrix  $\langle x|n\rangle$  and replacing  $\Phi \rightarrow x$  and  $\mathbf{P} \rightarrow -i\hbar\frac{d}{dx}$  we obtain the differential equation,

$$\begin{aligned} \hbar^2\sigma \left( n + \frac{1}{2} \right) \langle x|n\rangle &= \\ \left\{ (x - \phi)^2 \left( \eta^2 + \frac{\hbar^2\sigma^2}{\xi^2} \right) + \xi^2 \left( -i\hbar\frac{d}{dx} - p \right)^2 \right. \\ \left. - 2\xi\eta \left[ -i\hbar(x - \phi)\frac{d}{dx} - \frac{i\hbar}{2} - (x - \phi)p \right] \right\} \langle x|n\rangle \end{aligned} \quad (5.5)$$

which is easily solved in terms of the ordinary harmonic oscillator wavefunctions,

$$\psi_n(x; \omega) = \frac{1}{(2^n n!)^{\frac{1}{2}}} \left( \frac{\omega}{\pi\hbar} \right)^{\frac{1}{4}} H_n \left( \sqrt{\frac{\omega}{\hbar}} x \right) \exp \left( -\frac{\omega}{2\hbar} x^2 \right) \quad (5.6)$$

by

$$\langle x|n\rangle = \exp \left( \frac{ip(x - \phi)}{\hbar} + \frac{i\eta(x - \phi)^2}{2\hbar\xi} \right) \psi_n \left( x - \phi; \frac{\hbar\sigma}{2\xi^2} \right). \quad (5.7)$$

With the transformation matrix element determined it is a straightforward exercise in Gaussian integration and the properties of Hermite polynomials to obtain the form of the density matrix (3.16) in the time-independent number representation,

$$\begin{aligned} \langle n'|\rho|n\rangle &= \int_{-\infty}^{\infty} dx \int_{-\infty}^{\infty} dx' \langle n'|x'\rangle \langle x'|\rho|x\rangle \langle x|n\rangle \\ &= \frac{2\delta_{n'n}}{\sigma + 1} \left( \frac{\sigma - 1}{\sigma + 1} \right)^n, \end{aligned} \quad (5.8)$$

where  $\sigma$  is defined by (2.33). The derivation of these results and some further properties on the transformation matrices are given in Appendix B.

The matrix elements of the Liouville equation in this basis are

$$\begin{aligned} i\hbar\langle n|\dot{\rho}|n'\rangle &= \langle n|[H, \rho]|n'\rangle \\ &= (E_n - E_{n'})\langle n|\rho|n'\rangle. \end{aligned} \quad (5.9)$$

Clearly, if the density matrix in this basis is initially diagonal, which can always be accomplished by a Bogoliubov transformation (Appendix B), then it stays diagonal and time-independent. The time independence of the matrix elements of  $\rho$  in the Heisenberg number basis  $|n\rangle$  is simply a reflection of the fact that the density matrix (like the state vector  $|\psi\rangle$ ) is time independent in the Heisenberg picture where the field operator  $\Phi$  depends on time according to Eqn. (2.22). All the time-dependent dynamics resides in the transition matrix element  $\langle x|n\rangle$  which depends on the five variables  $(\phi(t), p(t); \xi(t), \eta(t); \sigma)$  while the matrix elements (5.8) remain forever unchanging under the mean field evolution. Indeed, this is just another reflection of the unitary Hamiltonian nature of the evolution, since the von Neumann entropy of the Gaussian density matrix

$$\begin{aligned} S &= -\text{Tr } \rho \ln \rho \\ &= \left(\frac{\sigma+1}{2}\right) \ln\left(\frac{\sigma+1}{2}\right) - \left(\frac{\sigma-1}{2}\right) \ln\left(\frac{\sigma-1}{2}\right) \\ &= (N+1) \ln(N+1) - N \ln N \end{aligned} \quad (5.10)$$

is strictly constant under the time evolution. Hence, there is no information lost in the evolution in any strict sense.

There is however another basis which is more appropriate for discussing ‘‘physical’’ particle number. This is the time-dependent Fock basis specified by replacing the mode function  $f$  which satisfies

$$\left(\frac{d^2}{dt^2} + \omega^2(t)\right) f(t) = \left(\frac{d^2}{dt^2} + \chi(t)\right) f(t) = 0 \quad (5.11)$$

by the adiabatic mode function,

$$\tilde{f}(t) \equiv \sqrt{\frac{\hbar}{2\omega(t)}} \exp\left(-i \int_0^t dt' \omega(t')\right), \quad (5.12)$$

and the Fock representation (5.2) by

$$\begin{aligned} \Phi(t) &= \tilde{a}(t)\tilde{f}(t) + \tilde{a}^\dagger(t)\tilde{f}^*(t), \\ \dot{\Phi}(t) = \mathbf{P}(t) &= -i\omega(t)\tilde{a}(t)\tilde{f}(t) + i\omega(t)\tilde{a}^\dagger(t)\tilde{f}^*(t), \end{aligned} \quad (5.13)$$

where the  $\tilde{a}$  and  $\tilde{a}^\dagger$  operators must now be time-dependent. The corresponding time-dependent number basis is defined by

$$\tilde{a}^\dagger \tilde{a} |\tilde{n}\rangle = \tilde{n} |\tilde{n}\rangle, \quad (5.14)$$

in which

$$\mathbf{H}_{osc} = \frac{\hbar\omega}{2}(\tilde{a}^\dagger \tilde{a} + \tilde{a} \tilde{a}^\dagger) \quad (5.15)$$

is diagonal for each time. In the  $\tilde{a}^\dagger \tilde{a}$  number basis,  $\rho$  is no longer diagonal,  $\langle \tilde{a} \rangle$ ,  $\langle \tilde{a} \tilde{a} \rangle$ , *etc.*, are non-vanishing, and  $\tilde{N} \equiv \langle \tilde{a}^\dagger \tilde{a} \rangle \neq N$  in general, except in the static case of constant  $\omega$ .

In addition to diagonalizing the time-dependent harmonic oscillator Hamiltonian  $\mathbf{H}_{osc}$  which describes the evolution of the Gaussian density matrix, the  $\tilde{n}$  basis has another important property, namely the existence of an adiabatic invariant  $W$ . This adiabatic invariant may be constructed from the Hamilton-Jacobi equation corresponding to the effective classical Hamiltonian  $H_{eff}$  in the usual way,

$$\frac{1}{2} \left(\frac{\partial W}{\partial x}\right)^2 + \frac{\omega^2}{2} x^2 + \frac{1}{2} \left(\frac{\partial W}{\partial \xi}\right)^2 + \frac{\omega^2}{2} \xi^2 + \frac{\hbar^2 \sigma^2}{8\xi^2} = E. \quad (5.16)$$

This equation is separable and the ansatz  $W(x, \xi) = W_1(x) + W_2(\xi)$  along with  $E = E_1 + E_2$  yields, in the first variable,

$$W_1 = \int dx \sqrt{2E_1 - \omega^2 x^2} = 2\pi \frac{E_1}{\omega} \quad (5.17)$$

while in the second variable  $\xi$  one obtains

$$W_2 = \int d\xi \sqrt{2E_2 - \omega^2 \xi^2 - \frac{\hbar^2 \sigma^2}{4\xi^2}}. \quad (5.18)$$

Under the substitution  $r = \xi^2/2$  this turns out to be the same integral which occurs in the Kepler problem, again pointing out the formal similarity with the angular momentum barrier in a central potential. Using standard methods [20], one finds

$$W_2 = 2\pi \frac{E_2}{\omega} - \pi \hbar \sigma. \quad (5.19)$$

Hence the full adiabatic invariant is

$$\frac{W}{2\pi\hbar} = \frac{E}{\hbar\omega} - \frac{\sigma}{2} = \tilde{N} - N. \quad (5.20)$$

upon using the definition of  $\tilde{N}$ , the definition of  $\sigma$  and

$$E = \langle \mathbf{H} \rangle = \langle \mathbf{H}_{osc} \rangle = \hbar\omega \left(\tilde{N} + \frac{1}{2}\right). \quad (5.21)$$

Since  $N$  is strictly a constant of the motion, Eqn. (5.20) informs us that  $\tilde{N}$  is an adiabatic invariant and therefore slowly varying if  $\omega^2 = \chi$  is a slowly varying function of time. In the language of classical action-angle variables,  $W$  is an action variable which is slowly varying while the angle variable conjugate to it varies rapidly in

time (linearly with time in the limit  $\omega$  is a constant, as in the exponent in (5.12)). This means that although the density matrix  $\rho$  is certainly not diagonal in the  $\tilde{n}$  number basis, its off-diagonal elements which depend on the angle variable will be very rapidly varying functions of time, whereas its diagonal elements in this basis will be only slowly varying. This is clearly seen in the explicit form for the matrix elements of this basis in Eqn. (B22) of Appendix B. Hence if we are interested only in the motion of the mean fields which are slowly varying functions of time we may average over the rapid phase variations in the off-diagonal matrix elements of  $\rho$  in this adiabatic number basis. For only a single quantum degree of freedom this amounts to a time-averaging, and can be implemented only by fiat. However in field theory there are many momentum modes, so that this averaging is actually performed for us in the mean field evolution equations by the integrations over  $k$  at fixed  $t$ .

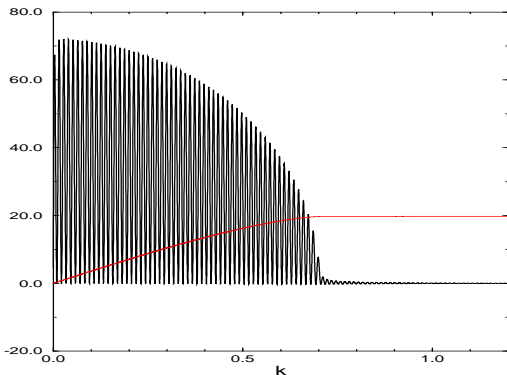


FIG. 8. Integrand and integral of the RHS of Eqn. (5.23) as a function of  $k$  for fixed  $t = 257$ .

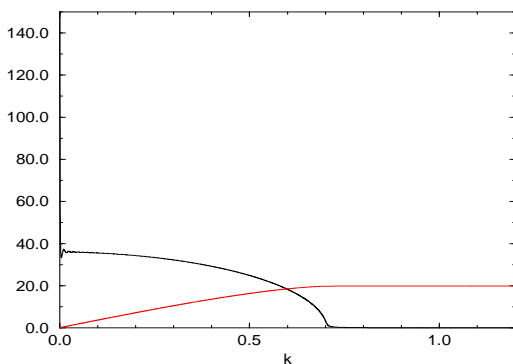


FIG. 9. Integrand and integral of the phase averaged quantity defined by the adiabatic particle number basis as a function of  $k$  for the same fixed  $t = 257$ . The value of the integral using the replacement (5.22) is the same as that of the previous figure.

The term *dephasing* has a precise meaning in this adi-

abatic particle number representation of the density matrix. To the extent that the phases in the off-diagonal matrix elements of the density matrix in the adiabatic  $\tilde{n}$  basis are rapidly varying in time, they should have little or no effect on the evolution of more slowly varying quantities such as the mean fields  $\phi$  and  $\chi$  or the mean adiabatic particle number  $\langle \tilde{N} \rangle$  itself. Thus, a natural approximation to the full density matrix  $\rho$  is immediately suggested by the existence of the adiabatic number basis, namely to discard the off-diagonal elements (see (B22) below) of  $\rho$  in this basis, which is equivalent to time-averaging the distribution of fluctuations in the exact Gaussian density matrix (3.30) over times long compared to their rapid variations. In field theory, where there are many Fourier modes, each with its own rapid phase variation, the effect of dephasing may be obtained by simply integrating over the momentum index  $k$  at fixed time. In either case, we expect this averaging procedure to scarcely affect the actual evolution of the mean fields, and the extent to which this expectation is realized is the extent to which dephasing of the fluctuations is effective, and the evolution is irreversible. In Figs. 8 and 9 we compare the actual  $k$  dependence of the function  $G(k, t)$  appearing in the mean field evolution equation (2.13) with the phase averaged quantity defined by the adiabatic particle number  $\tilde{N}(k)$ , *i.e.* we make the replacement,

$$-i\hbar G(k, t) = |f_k(t)|^2 \rightarrow \frac{1}{2k}(2\tilde{N}(k) + 1). \quad (5.22)$$

The relevant integral in the renormalized gap equation (2.34) is

$$G(x, x, \chi) - G(x, x, \chi = 0) = \frac{1}{4\pi^2} \int_0^\Lambda k^2 dk \left\{ |f_k(t)|^2 \sigma_k - \frac{\hbar}{2k} \right\}. \quad (5.23)$$

Notice that although there are many more oscillations in the integrand of the RHS of Eqn. (5.23) than in the phase averaged quantity, the integrals over  $k$  of the two quantities are indistinguishable.

The adiabatic particle basis may also be used to define effective Boltzmann and von Neumann entropies [21] through the diagonal matrix elements (B22) below. Neglecting the rapidly varying off-diagonal matrix elements gives

$$S_B \equiv \sum_{\vec{k}} \left\{ (\tilde{N}(\vec{k}) + 1) \ln (\tilde{N}(\vec{k}) + 1) - \tilde{N}(\vec{k}) \ln \tilde{N}(\vec{k}) \right\}$$

$$S_{eff} \equiv -\text{Tr} \rho_{eff} \ln \rho_{eff}$$

$$= - \sum_{\vec{k}} \sum_{\ell=0}^{\infty} \rho_{2\ell}(\vec{k}) \ln \rho_{2\ell}(\vec{k}) \quad (5.24)$$

for the Boltzmann and effective von Neumann entropy of the truncated density matrix, where  $\rho_{2\ell}(\vec{k})$  is given by Eqn. (5.25) below. The evolution of these two quantities for a typical solution of the mean field equations is shown

in Fig. 10. Both display general increase due to continuous creation of massless Goldstone particles near threshold [22]. Neither quantity is a strictly monotonic function of time and neither obeys a strict Boltzmann  $H$ -theorem. Since the particle modes  $f_k$  interact with the mean field  $\chi$  but not directly with each other, the effective damping observed is certainly *collisionless*, and the dephasing here is similar to that responsible for Landau damping of collective modes in classical electromagnetic plasmas. The entropy  $S_{eff}$  of the effective density matrix provides a precise measure of the information lost by treating the phases as random. The Boltzmann “entropy” would be expected to equal  $S_{eff}$  only in true thermodynamic equilibrium, which is not achieved in the collisionless approximation of Eqns. (2.20). Notice the non-thermal distribution of particles in Fig. 9. In this non-thermal distribution we see from Fig. 10 that the Boltzmann entropy  $S_B$  generally overestimates the amount of information lost by phase averaging.

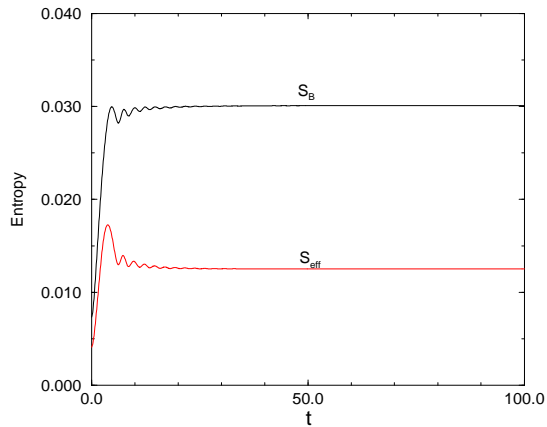


FIG. 10. Evolution of the Boltzmann and effective von Neumann entropies of the diagonal elements of the density matrix in the adiabatic particle number basis.

To the extent that the phase information in the off-diagonal matrix elements of  $\rho$  is irretrievable the system has become effectively classical, in the sense that the quantum interference effects present in the original ensemble represented by  $\rho$  are washed out as well. In that case we might as well regard the ensemble represented by the diagonal, truncated effective density matrix in the adiabatic number basis as a *classical* probability distribution with the diagonal elements of  $\langle \tilde{n} = 2\ell | \rho | \tilde{n} = 2\ell \rangle$  giving the classical probabilities of observing  $\ell$  pairs in the ensemble. This probability distribution is derived in Appendix B and given by

$$\begin{aligned} \rho_{2\ell}(\vec{k}) &= \langle \tilde{n}_{\vec{k}} = 2\ell | \rho | \tilde{n}_{\vec{k}} = 2\ell \rangle \Big|_{\substack{\sigma=1 \\ \phi=\phi=0}} \\ &= \frac{(2\ell - 1)!!}{2^\ell \ell!} \operatorname{sech} \gamma_{\vec{k}} \tanh^{2\ell} \gamma_{\vec{k}} \end{aligned} \quad (5.25)$$

where  $\gamma$  is the magnitude of the Bogoliubov transforma-

tion between the  $a$  and  $\tilde{a}$  bases, given explicitly in terms of the mode functions by

$$\tilde{N}(\vec{k}) = \sinh^2 \gamma_{\vec{k}} = \frac{|\dot{f}_k + i\omega_k f_k|^2}{2\hbar\omega_k}, \quad (5.26)$$

which depends only on the magnitude of  $\vec{k}$  by spatial homogeneity. Sampling this distribution with random phases will yield typical classical field amplitudes which make up the distribution. Obtaining such typical classical fields in the ensemble can give us explicit realizations of the symmetry breaking behavior of the system, as well as providing the starting point for the study of topological defects produced during the phase transition.

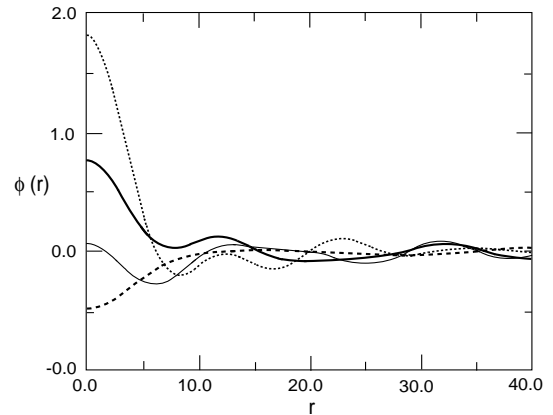


FIG. 11. Four typical field configurations drawn from the same classical distribution of probabilities in the adiabatic particle number basis, according to Eqn. (5.30), for  $t=490$  in the case the mean field  $\phi = 0$ . The units of  $r$  are  $v^{-1}$  and  $\lambda_\Lambda = 1$ .

The sampling of the field configurations proceeds in several steps. For a fixed late time and Fourier wave number  $k$  we calculate the Bogoliubov transformation coefficient from the static  $n$  to time-dependent adiabatic particle number  $\tilde{n}$  basis from Eqn. (5.26). This gives a set of numbers  $\rho_{2\ell} = \langle \tilde{n} = 2\ell | \rho | \tilde{n} = 2\ell \rangle$  normalized to unit total probability,

$$\sum_{\ell=0}^{\infty} \rho_{2\ell} = 1 \quad (5.27)$$

and which typically fall off very rapidly with  $\ell$  so that only a finite number of the  $\rho_{2\ell}$  need be retained. Then we sample this distribution by drawing a random number  $q$  in the unit interval  $[0, 1]$ . Looking at the table of  $\rho_{2\ell}$  and the partial sums,

$$Q_\ell = \sum_{\ell'=0}^{\ell} \rho_{2\ell'} \quad (5.28)$$

we find  $\ell$  such that

$$Q_{\ell-1} < q \leq Q_\ell \quad (5.29)$$

to determine  $\tilde{n} = 2\ell$  of this random drawing for the given value of  $k$ . We then write

$$\begin{aligned} \phi(r, t) &= \frac{1}{\sqrt{V}} \sum_{\mathbf{k}} \frac{1}{\sqrt{2\omega_{\mathbf{k}}}} (a_{\mathbf{k}} e^{i\mathbf{k}\cdot\mathbf{x}} + a_{\mathbf{k}}^* e^{-i\mathbf{k}\cdot\mathbf{x}}) \\ &\rightarrow \frac{\sqrt{V}}{\pi^2 r} \int_0^\infty dk k \sin kr \sqrt{\frac{\tilde{n}_k}{2\omega_k}} \cos \theta_k, \end{aligned} \quad (5.30)$$

where we have performed the angular integrations in  $d = 3$  dimensions, and written

$$a_k = \sqrt{\tilde{n}_k} e^{i\theta_k} \quad (5.31)$$

in terms of a random phase  $\theta_k$ . After performing the Fourier transform in (5.30) the result is a typical field configuration as a function of radial  $r$  at the fixed time  $t$ . In this way we obtained the four field configurations shown in Fig. 11. We observe that although the mean field  $\phi = 0$  when averaged over the entire ensemble, typical field configurations in the ensemble are quite far from zero. In fact they sample values of  $\phi$  between the two minima at  $v$  and  $-v$ . We observe as well that there is a typical correlation length in the classical field configurations which is of the order of the inverse momentum in which the power of the two-point function is distributed, as in Fig. 9.

It is clearly possible by such sampling techniques to generate typical field configurations with any number of components  $\Phi_i$  in any number of spatial dimensions  $d$ . Then by appropriately matching the number of components to the number of dimensions we could search for different types of defect-like structures such as vortices, strings, and domain walls. This classical description of the quantum mean field theory is possible only when a classical decoherent limit exists through the diagonal density matrix in the adiabatic particle number basis. Moreover, the classical fields generated by this procedure are smooth and free of any cut-off dependent short distance effects. The extraction of smooth classical field configurations from a quantum mean field description is a direct consequence of dephasing and the definition of defect number in these smooth configurations is free of the difficulties encountered when classical definitions of defects are applied uncritically to quantum field theories. It would be very interesting to pursue these ideas further in more realistic models of phase transitions where such topological defects are expected. This we leave for a future investigation.

The dephasing of the density matrix justifies the replacement of the exact Gaussian  $\rho$  by its diagonal elements only in the adiabatic number basis leading to the effective density matrix  $\rho_{eff}$ . Now if this effective density matrix is transformed back into the coordinate basis it corresponds to a density matrix of the original Gaussian form but with zero mean fields, zero momentum  $\eta_k = 0$  and  $\tilde{\sigma}_k \equiv 1 + 2\tilde{N}(k)$  replacing  $\sigma$ , *i.e.* we obtain a product of Gaussians of the form,

$$\begin{aligned} \langle \varphi'_k | \rho_{eff} | \varphi_k \rangle &= \\ (2\pi\xi_k^2)^{-\frac{1}{2}} \exp \left\{ -\frac{\tilde{\sigma}_k^2}{8\xi_k^2} (\varphi'_k - \varphi_k)^2 - \frac{1}{8\xi_k^2} (\varphi'_k + \varphi_k)^2 \right\}, \end{aligned} \quad (5.32)$$

in all the  $k \neq 0$  modes where the mean field vanishes. This form shows that the Gaussian distribution off the diagonal  $\varphi'_k = \varphi_k$  is strongly suppressed compared to the diagonal distribution. Indeed in the numerical evolutions we have found that  $k\tilde{N}(k)$  behaves like a constant for small  $k$ . This means that  $\tilde{\sigma} \propto 1/k$  which is large for small  $k$ . Hence whereas the root mean square deviation from zero along the diagonal  $\varphi'_k = \varphi_k$  is  $\xi_k \cong \sqrt{\hbar\tilde{N}(k)}/k$  which is large, the root mean square deviation from zero in the orthogonal direction off the diagonal is

$$\frac{\xi_k}{\sigma_k} \cong \sqrt{\frac{\hbar}{2k\tilde{N}(k)}}$$

which is much smaller. The result is that there is virtually no support in this distribution for ‘‘Schrödinger cat’’ states in which quantum interference effects between the two classically allowed macroscopic states at  $v$  and  $-v$  can be observed. Instead we see in a different way how dephasing produces an ensemble which may be regarded as a classical probability distribution over classically distinct outcomes (*i.e.* the diagonal field amplitude distribution) but with essentially no components in the off-diagonal quantum interference between these classical configurations. This is illustrated in Fig. 12. Hence even in this rather simple collisionless approximation the particle creation effects in the time dependent mean field give rise to strong suppression of quantum interference effects and mediate the quantum to classical transition of the ensemble.

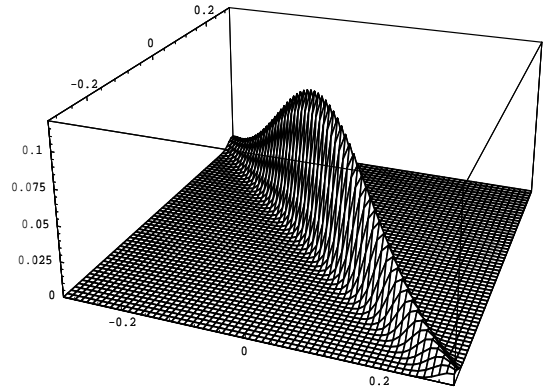


FIG. 12. The Gaussian  $\rho_{eff}$  for  $k = .4$  for the data and parameter values of Fig. 9 illustrating the strong suppression of off-diagonal components due to dephasing.

When more realistic collisional interactions are included at the next and higher orders beyond the leading mean field limit we can expect this transition to decoherent classical behavior to be even more pronounced. As

the Gaussian assumption is relaxed we expect the single peak at the origin to split into two peaks. Hence we can begin to see how a quantum phase transition leads to an effective classically broken symmetry in which large domains are in a definite classical ground state or another but not in a quantum superposition of ground states.

## VI. LINEAR RESPONSE, PLASMA OSCILLATIONS AND DAMPING RATE

The very efficient damping of the oscillations around the final state which we have studied in the density matrix formalism of the last section may also be understood as due to the continuous creation of massless Goldstone particles near threshold. In this appearance of strictly massless modes the spontaneously broken  $\lambda\Phi^4$  model is qualitatively different from our previous studies of QED in the large  $N$  approximation [23]. In that case the charged particles are massive and there is finally a tunneling barrier which shuts off particle creation effects after the mean electric field has decreased below a certain critical value. Beyond this point the mean field undergoes essentially undamped plasma oscillations since there is no transfer of energy to created particles. In contrast, the present model has no such critical threshold in the mean field  $\chi$  which is free to continue creating massless bosons for arbitrarily small amplitude and  $\chi \rightarrow 0$  asymptotically. This very efficient asymptotic damping of the  $\chi$  mean field towards its stationary spontaneously broken solution at  $\chi = 0$  is very well illustrated by the numerical results shown in Figs. 13 and 14 for  $\lambda_\Lambda = 1$  and an initial  $\chi = -.5$

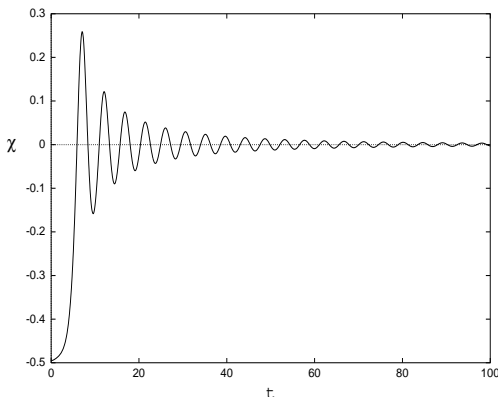


FIG. 13. Time evolution and effective damping of the  $\chi$  mean field towards zero, its stationary value in the spontaneously broken phase.

Since  $\chi$  becomes very small at late times, it is possible to analyze the approach to zero by linear response methods. In principle this is possible for any initial condition but we restrict ourselves to the thermal and vacuum cases. With thermal initial conditions, both the fre-

quency and the damping rate of the plasma oscillations can be calculated and are in very good agreement with the simulations as will be discussed further below. The long time behavior for initial conditions with  $N(k) = 0$  is somewhat more complicated. While the oscillation frequency is still very well determined by the linear response analysis, the oscillation envelope does not damp exponentially. Instead it falls off as an exponential multiplied by a power law in time.

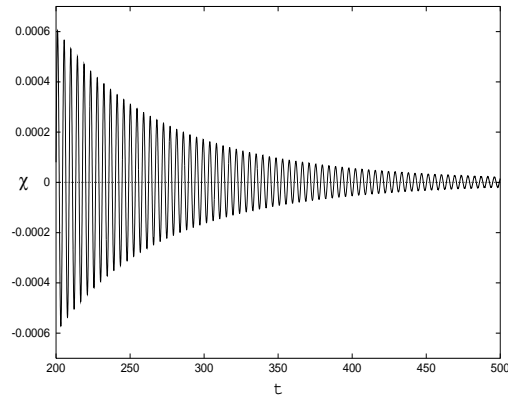


FIG. 14. Same evolution as in Fig. 13 but followed to large times and with an expanded scale for  $\chi$  to show the long time behavior of the time-dependent Goldstone mass squared.

Given any static solution to the equations of motion with spontaneous symmetry breaking, as in (4.18), we may consider the real time linear response of the system away from this static solution. This is accomplished by linearizing the evolution equations in the deviations from the static solution,

$$\begin{aligned}\phi &\rightarrow \phi + \delta\phi \\ \chi &\rightarrow 0 + \chi \\ f_k &\rightarrow f_k(t) + \delta f_k(t),\end{aligned}\quad (6.1)$$

with

$$f_k(t) = \sqrt{\frac{\hbar}{2k}} \exp(-ikt) \quad (6.2)$$

the mode functions corresponding to the static solution,  $\chi = 0$ .

The linearized mode equation,

$$\left[ \frac{d^2}{dt^2} + k^2 \right] \delta f_k(t) = -\chi(t) f_k(t) \quad (6.3)$$

may be solved by use of the retarded Green's function,

$$G_R(t-t'; k) = \frac{\sin k(t-t')}{k} \theta(t-t') \quad (6.4)$$

in the form,

$$\begin{aligned}\delta f_k(t) &= A_k f_k(t) + B_k f_k^*(t) \\ &\quad - \int_0^t dt' G_R(t-t'; k) \chi(t') f_k(t')\end{aligned}\quad (6.5)$$

where  $A_k$  and  $B_k$  are coefficients of the solutions to the homogeneous equation. Because the Wronskian condition (2.26) is maintained under the linearization, the  $A_k$  must have vanishing real part,

$$\text{Re } A_k = 0 . \quad (6.6)$$

The linearized  $\phi$  equation gives in the same way,

$$\begin{aligned} \delta\phi(t) &= t \delta\dot{\phi}(0) + \delta\phi(0) \\ &- \int_0^t dt' G_R(t-t'; k=0) \chi(t') \phi(t') . \end{aligned} \quad (6.7)$$

At the same time the linearized gap equation reads

$$\chi = \lambda\phi \delta\phi + \lambda \int [d\mathbf{k}] \text{Re}(\delta f_k f_k^*) (1 + 2N(k)) . \quad (6.8)$$

Upon substituting Eqns. (6.5-6.7) this becomes a linear integral equation for the perturbation,  $\chi$ ,

$$\chi(t) = -\lambda \int_0^t dt' \Pi(t-t') \chi(t') + \lambda B(t) , \quad (6.9)$$

where

$$\Pi(t) = t\phi^2 + \int [d\mathbf{k}] \frac{(1 + 2N(k))}{2k^2} \sin kt \cos kt \quad (6.10)$$

is the polarization part in the static background and

$$\begin{aligned} B(t) &\equiv t\phi \delta\dot{\phi}(0) + \phi\delta\phi(0) \\ &+ \int [d\mathbf{k}] \frac{(1 + 2N(k))}{2k} \text{Re}(B_k e^{2ikt}) \end{aligned} \quad (6.11)$$

depends only on the initial perturbation away from the static solution. The linearized integral equation (6.9) may be put in the form

$$\int_0^t dt' D^{-1}(t-t') \chi(t') = -B(t) \quad (6.12)$$

where  $D^{-1}$  the  $\chi$  inverse propagator function.

The most direct method of solving such integral equations is to make use of the Laplace transforms,

$$\begin{aligned} \tilde{\Pi}(s) &\equiv \int_0^\infty dt e^{-st} \Pi(t) \\ &= \frac{\phi^2}{s^2} + \int [d\mathbf{k}] \frac{(1 + 2N(k))}{2k(s^2 + 4k^2)} , \\ \tilde{B}(s) &\equiv \int_0^\infty dt e^{-st} B(t) \\ &= \frac{\phi \delta\dot{\phi}(0)}{s^2} + \int [d\mathbf{k}] \frac{(1 + 2N(k))}{2k} \text{Re} \left( \frac{B_k}{s - 2ik} \right) , \\ \tilde{\chi}(s) &\equiv \int_0^\infty dt e^{-st} \chi(t) = -\tilde{D}(s) B(s) , \end{aligned} \quad (6.13)$$

and  $\tilde{D}(s)$ , the simple algebraic reciprocal of the Laplace transform of  $D^{-1}(t)$ ,

$$-\tilde{D}^{-1}(s) = \frac{1}{\lambda} + \tilde{\Pi}(s) = \frac{1}{\lambda} + \frac{\phi^2}{s^2} + \int [d\mathbf{k}] \frac{(1 + 2N(k))}{2k(s^2 + 4k^2)} . \quad (6.14)$$

Both the bare coupling  $\lambda = \lambda_\Lambda$  and the integral over  $\mathbf{k}$  involving the  $N(k)$  independent term are logarithmically divergent. They combine to give the ultraviolet finite contribution,

$$\begin{aligned} \frac{1}{\lambda_R(s^2/4)} &= \frac{1}{\lambda_\Lambda} + \frac{\hbar}{32\pi^2} \ln \left( \frac{4\Lambda^2}{s^2} \right) \\ &= \frac{1}{\lambda_R(m^2)} + \frac{\hbar}{32\pi^2} \ln \left( \frac{4m^2}{s^2} \right) . \end{aligned} \quad (6.15)$$

The renormalized sum rule (4.19) may be used in the  $N(k)$  dependent term to secure as well

$$\begin{aligned} -\tilde{D}^{-1}(s) &= \frac{1}{\lambda_R(s^2/4)} + \frac{v^2}{s^2} \\ &+ \frac{\hbar}{2\pi^2} \int_0^\infty k dk N(k) \left( \frac{1}{s^2 + 4k^2} - \frac{1}{s^2} \right) \end{aligned} \quad (6.16)$$

which is now independent of the static value of  $\phi$ .

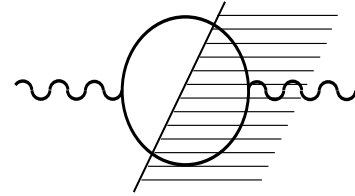


FIG. 15. One loop diagram which contributes to the polarization  $\Pi = -\frac{i}{2} G G$  in the leading order large  $N$  approximation.

The function  $\tilde{D}^{-1}(s)$  has a singularity at  $s = 0$  and depending on the exact form of  $N(k)$  near  $k = 0$  in general, a branch cut starting from the origin in the complex  $s$  plane which may be taken along the negative real  $s$  axis. Its physical origin is the zero mass Goldstone bosons propagating in the internal loop of the polarization  $\Pi$  in Fig. 15. The discontinuity across this cut arises from the non-zero probability for the time dependent  $\chi$  field to create Goldstone pairs with arbitrarily small spatial momentum  $k$  above the massless threshold. The function  $\tilde{D}^{-1}(s)$  also may have one or more zeroes in the left-half complex  $s$  plane. The zero at

$$s^2 \cong \pm 4m^2 \exp \left( \frac{32\pi^2}{\hbar\lambda_R(m^2)} \right) \rightarrow \pm\infty \quad (6.17)$$

for  $\lambda_R \ll 1$  is the Landau ghost pole in the far ultraviolet which lies outside the range of validity of the large  $N$  expansion and which in any case does not affect the long-time behavior of the inverse Laplace transform.

In the case of a strictly thermal distribution of massless bosons (3.15), the integral in (6.16) may be performed in

closed form in terms of the digamma function  $\psi$  and we find

$$\begin{aligned} -\tilde{D}_T^{-1}(s) &= \frac{1}{\lambda_R(s^2/4)} + \frac{\phi_T^2}{s^2} \\ &\quad + \frac{\hbar}{16\pi^2} \left[ \ln\left(-\frac{s}{4\pi T}\right) + \frac{2\pi T}{s} - \psi\left(\frac{-s}{4\pi T}\right) \right] \\ &= \frac{1}{\lambda_R(4\pi^2 T^2)} + \frac{\phi_T^2}{s^2} \\ &\quad + \frac{\hbar}{16\pi^2} \left[ \frac{2\pi T}{s} - \psi\left(-\frac{s}{4\pi T}\right) \right]. \end{aligned} \quad (6.18)$$

A particular case is  $T = 0$  in which case the integral vanishes and  $\tilde{D}_0^{-1}(s)$  possesses a zero at complex  $s_{\pm}$  in the left-hand complex plane,

$$s_{\pm} = \pm i\omega - \gamma \quad (6.19)$$

with

$$\begin{aligned} \omega^2 &\cong \lambda_{pl} v^2 \quad \text{and} \\ \gamma &\cong \frac{\lambda_{pl}}{64\pi} \omega = \frac{\lambda_{pl}^{\frac{3}{2}}}{64\pi} v \end{aligned} \quad (6.20)$$

where

$$\lambda_{pl} = \lambda_R(s^2/4 = -\omega_{pl}^2/4), \quad (6.21)$$

for  $\lambda_{pl} \ll 1$ . In the frequency (6.20) the effective mass of the ‘‘radial’’ mode, ignored in the direct quantization of the  $N - 1$  massless modes in (2.22) reappears in the large  $N$  limit as an oscillation in the real time linear response to perturbations about the vacuum  $\phi = v$ ,  $\chi = 0$ . It may be viewed either as this radial degree of freedom of the  $N$  component  $\Phi_i$  field, with its effective mass dressed by the polarization effects of  $\Pi$  in the presence of massless Goldstone modes, or alternately and just as correctly, as a genuine collective excitation of the composite field  $\chi$ . The two descriptions are equivalent since the oscillations of  $\chi$  and  $\phi$  are constrained by the linearized equations (6.7) and (6.8), and there is only one degree of freedom between them. The oscillation frequency (6.20) should be compared with the second derivative of the free energy potential at  $T = 0$  which vanishes from Eqn. (4.11). Thus the ‘‘effective’’ potential is completely ineffective at predicting the radial oscillation frequency at zero temperature. It is clear that at zero temperature the origin of the decay rate  $\gamma$  is the imaginary part of the two-particle cut in the polarization diagram illustrated in Fig. 16.

At finite temperature the analytic structure of  $\tilde{D}_T^{-1}(s)$  in the complex plane with  $\text{Re } s < 0$  is as anticipated on general physical grounds, *i.e.* there is a logarithmic branch cut beginning at  $s = 0$  along the negative real  $s$  axis with a discontinuity that monotonically increases from zero to its asymptotic value of  $\pm i\hbar/32\pi$  from the logarithm in (6.15) as  $s$  runs from 0 to  $-\infty$ . Indeed, the digamma function of small argument behaves like

$$\psi(z) \equiv \frac{d \ln \Gamma(z)}{dz} \rightarrow -\frac{1}{z} - \gamma_E \quad \text{as } z \rightarrow 0 \quad (6.22)$$

where  $\gamma_E = 0.577215\dots$  is Euler’s constant, so that we see from the second form of (6.18) that the logarithms cancel and the discontinuity vanishes, leaving a simple pole structure,

$$-\tilde{D}_T^{-1}(s) \rightarrow \frac{1}{\lambda_{R,T}} + \frac{\phi_T^2}{s^2} - \frac{T}{8\pi s} \quad (6.23)$$

as  $s \rightarrow 0$ . Setting this to zero and solving the quadratic equation informs us that  $\tilde{D}_T^{-1}(s)$  has a zero at  $s_{\pm}$  as in (6.19) with

$$\begin{aligned} \omega_{plT}^2 &= \lambda_R(T'^2) \phi_T^2 \quad \text{and} \\ \gamma_T &= \frac{\lambda_R(T'^2)}{16\pi} T \end{aligned} \quad (6.24)$$

for  $|s_{\pm}| \ll T$  and  $T' \equiv 2\pi e^{-2\gamma_E} T$ . This condition implies that Eqn. (6.24) is only valid in the critical region,

$$\left(\frac{T_c - T}{T_c}\right)^2 \ll \frac{T^2}{\hbar \lambda_R T_c^2} \quad (6.25)$$

where one would legitimately question the validity of the leading order mean field approximation. The approach of  $\omega_{plT}^2$  to zero as  $T \rightarrow T_c$  is a manifestation of critical slowing down. Notice also that this near critical temperature plasma oscillation (6.24) does not go over smoothly to the zero temperature case (6.20) since opposite limits of the digamma function are involved, and  $T \rightarrow 0$  is not permitted in Eqn. (6.24) without violating the assumption  $|s_{\pm}| \ll T$ . However, it seems likely that the simple poles found at zero temperature migrate continuously from their location at  $s_{\pm}$  given by (6.20) to the negative real axis as in (6.24) as the temperature is raised from zero to  $T_c$ . It would be interesting to map out the analytic structure of  $\tilde{D}_T^{-1}(s)$  in the left half complex  $s$  plane as a function of  $T$  to study the intermediate temperature behavior of the linear response function from its low temperature form to the critical region, without recourse to the asymptotic expansion (6.22). We reiterate that  $\tilde{D}_T^{-1}(s)$  describes the real time oscillations of the  $\phi$  mean field coupled to the collective plasma oscillations of the auxiliary field  $\chi$ , and that the equilibrium free energy ‘‘effective’’ potential  $F$  has no such real time information at either zero or finite temperature, as conclusively demonstrated by (4.11).

The linear response predictions for the oscillation frequency and the damping rate in the case of finite temperature were compared with a numerical evolution with  $\lambda_{\Lambda} = .01$  and  $T = 1$ . The theoretical predictions of  $\omega_{plT} = .09574$  and  $\gamma_T = 1.9894 \times 10^{-4}$  are in very good agreement with the numerical results  $\omega_{plT} = .09585$  and  $\gamma_T = 2 \times 10^{-4}$ . A similar test was carried out at a larger value of the coupling  $\lambda_{\Lambda} = .1$  again with excellent results: predictions of  $\omega_{plT} = 0.3028$  and  $\gamma_T = 1.9894 \times 10^{-3}$  compared with numerical values of  $\omega_{plT} = 0.3031$  and

$\gamma_T = 1.9944 \times 10^{-3}$ . The extraction of the behavior of the  $\chi$  envelope from the numerical data is described below.

Instead of plotting  $\chi$  directly as a function of time, information may be extracted more conveniently by plotting

$$y_t \equiv \frac{\log(y(t + \epsilon)) - \log(y(t))}{\log(t + \epsilon) - \log(t)} \quad (6.26)$$

as a function of time, where each time point  $t$  is taken at either a peak or a trough of the oscillation and  $\epsilon$  is the time separation between two such neighboring points. At late times, if the frequency stabilizes,  $\epsilon$  goes to a constant. Using this fact, along with the late time condition  $t \gg \epsilon$ , one can show from (6.26) that if the  $\chi$  oscillation envelope can be fit by an expression of the form

$$At^{-\alpha} \exp -\gamma t, \quad (6.27)$$

then at late times,

$$y_t = -\gamma t - \alpha, \quad (6.28)$$

enabling the direct reading off of the power  $\alpha$  and the exponent  $\gamma$  as the  $y$ -intercept and slope of a straight line respectively. It is important to note that this method is also a test of whether the frequency is stable as otherwise a straight line will not be obtained. The behavior of  $y_t$  against time is shown in Fig. 17 for the two values of the coupling constant mentioned above.

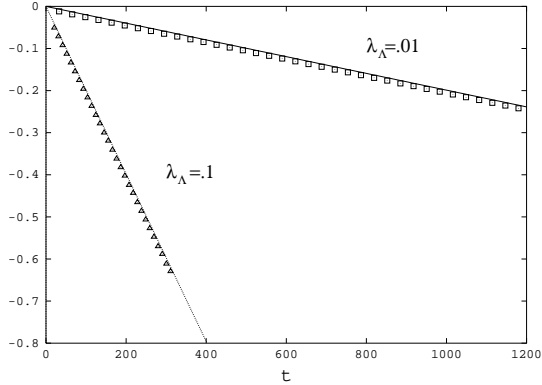


FIG. 16. The function  $y_t$  defined in Eqn. (6.26) plotted for perturbed thermal initial conditions at two values of  $\lambda_A$ . The solid lines are the corresponding theoretical predictions.

When the distribution  $N(k)$  is non-thermal the behavior of  $\tilde{D}^{-1}(s)$  is more difficult to analyze, and there is no guarantee that it possesses a zero in general. If  $N(k)$  is peaked at small  $k$  then a reasonable first approximation is to neglect the last term in (6.16). In that case we find a zero of  $\tilde{D}^{-1}(s)$  at with

$$\begin{aligned} \omega_{pl}^2 &\approx \lambda_{pl} v^2 & \text{and} \\ \gamma &\approx \frac{\lambda_{pl}}{64\pi} \omega_{pl} = \frac{\lambda_{pl}^{\frac{3}{2}} v}{64\pi}. \end{aligned} \quad (6.29)$$

If the running renormalized  $\lambda_R$  is not very small and/or  $N(k)$  is not sharply peaked at  $k = 0$  then the position of this zero of  $\tilde{D}^{-1}(s)$  will be shifted from (6.29), and at some values it may even cease to exist. Comparing with our numerical data for which  $k\tilde{N}(k)$  is shown in Fig. 18, we observe that the approximations leading to the estimates (6.29) can only be order of magnitudes at best. Indeed the numerical value of the plasma frequency from the data at late times is  $\omega_{pl} = 1.405$  whereas (6.29) gives  $\omega_{pl} = v$ . The damping rate is estimated to be  $\gamma = 0.005v$  (or  $0.007v$  if the correct  $\omega_{pl}$  is used), however the envelope of the oscillations at late times is not even strictly exponential as we shall see below. Hence we cannot expect to obtain an accurate estimate of the damping rate by a simple pole analysis of the Laplace transform  $\tilde{D}(s)$ . Nevertheless, if one fits an exponential to the data at late times a value  $\gamma = 0.009v$  is obtained, agreeing only roughly with the estimate.

Despite the envelope of the oscillations being non-exponential,  $\omega_{pl}$  is very well determined by the regular oscillations observed (to a few parts in  $10^3$ ). To obtain a more accurate approximation to the plasma frequency consider the following analytic approximation to  $kN(k)$ ,

$$kN(k) = 8\pi\omega_0 \theta(\omega_0^2 - 4k^2) \sqrt{1 - \frac{4k^2}{\omega_0^2}}, \quad (6.30)$$

where  $\omega_0$  is a free parameter which is close to the numerical value of the plasma frequency. The accuracy of this analytic fit to the data is shown in Fig. 18 for  $\omega_0 = \omega_{pl}$ . Notice that because of dephasing, the  $N(k)$  of the initial state in the linear response analysis may be identified with the  $\tilde{N}(k)$  of the particles created earlier in the non-linear evolution from the spinodal region (except for very small  $k < 1/t$  where the dephasing is as yet ineffective).

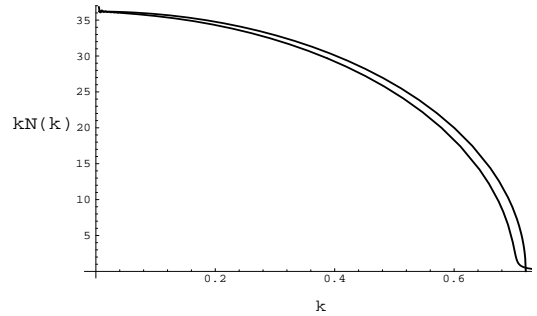


FIG. 17. Comparison of the analytic approximation to the particle number density of Eqn. (6.30) (upper curve) with the adiabatic number density of the numerical calculation (bottom curve).

Substituting the form (6.30) into (6.16) we obtain

$$\begin{aligned} -\tilde{D}^{-1}(s) &= \frac{1}{\lambda_R(s^2/4)} + \frac{v^2}{s^2} \\ &+ \frac{2\omega_0^2}{\pi} \int_0^1 dy (1-y^2)^{\frac{1}{2}} \left[ \frac{1}{\omega_0^2 y^2 + s^2} - \frac{1}{s^2} \right]. \end{aligned} \quad (6.31)$$

Because of the small prefactor of the logarithm in  $1/\lambda_R(s^2/4)$ , the running coupling constant is only a few percent different from the bare  $\lambda$  near the zero of  $\tilde{D}^{-1}(s)$  and this running with  $s$  can be neglected in lowest order. Again we set  $s = \pm i\omega_{pl} - \gamma$  and look for a zero of  $D^{-1}(s)$  near  $\omega_0^2 = \omega_{pl}^2$ , with  $\gamma/\omega \ll 1$ . One could perform the integral in (6.31) exactly but we content ourselves with this simple approximation and obtain

$$0 \cong \frac{1}{\lambda_{pl}} - \frac{v^2}{\omega_0^2} + \frac{2}{\pi} \int_0^1 dy [(1-y^2)^{\frac{1}{2}} - (1-y^2)^{-\frac{1}{2}}]. \quad (6.32)$$

Performing the integral we find from the real part of this equation,

$$\frac{\omega_{pl}^2}{v^2} = \frac{2\lambda_{pl}}{2 - \lambda_{pl}} \quad (6.33)$$

In our simulations where  $\lambda_\Lambda = 1 \simeq \lambda_{pl}$ , the output value of the calculated plasma oscillation frequency  $\omega_{pl} = 1.414v$  is within 0.6% of the measured value  $\omega_{pl} = 1.405v$  showing the self-consistency of the approximation and the fit (6.30), to this accuracy. We also performed the integration in (6.16) numerically using the data of Fig. 18 for  $kN(k)$  and reconfirmed  $\omega_{pl} = (1.405 \pm 0.001)v$  from the location of the minimum of the real part of  $\tilde{D}^{-1}(s)$ .

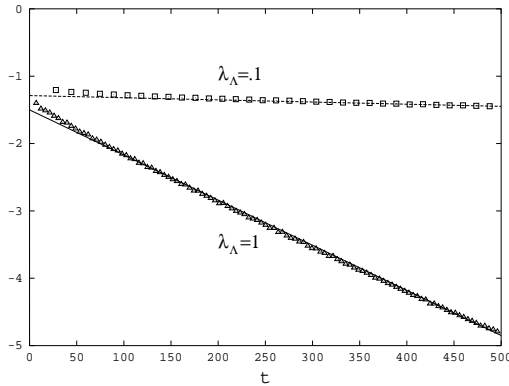


FIG. 18. The function  $y_t$  plotted for  $N(k) = 0$  initial conditions at two values of  $\lambda_\Lambda$ . The late time linear fits to the data are also shown with the intercepts determining the power law prefactor.

The envelope of the  $\chi$  oscillations obtained numerically is very well fit by  $t^{-\alpha} \exp(-\gamma t)$ . This general behavior has been checked for different values of the bare coupling and we have verified that it does not depend on which choice of the  $\omega_k$  profiles (C4) and (C5) one makes for the initial conditions. Illustrated in Fig. 19 are the  $\lambda_\Lambda = 1$  and  $\lambda_\Lambda = .1$  cases, where  $\alpha = 1.5$ ,  $\gamma = .0067$  and  $\alpha = 1.288$ ,  $\gamma = .00032$  respectively. Figs. 19 and 20

display the complete fit to the damped oscillation alongside the actual evolution for the case  $\lambda_\Lambda = 1$ . Very good agreement is evident over long times and large amplitude range. The case of  $\lambda_\Lambda = .1$  is very similar.

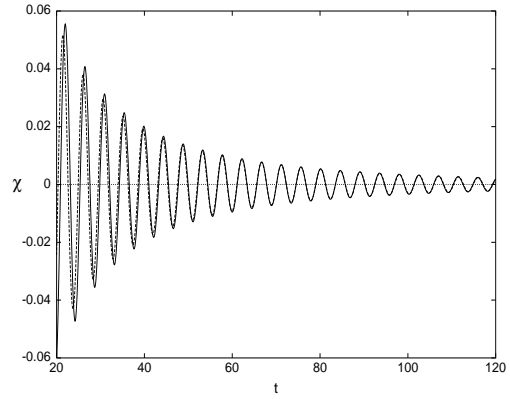


FIG. 19. The  $\chi$  evolution as a function of time (dashed line) for  $\lambda_\Lambda = 1$ . The fit (6.27), shown by the solid curve is  $\chi(t) = 6.63t^{-1.5} \exp(-.0067t) \cos(1.405t + .5)$ . This figure shows the fit over an early time range,  $t = 20, 120$ .

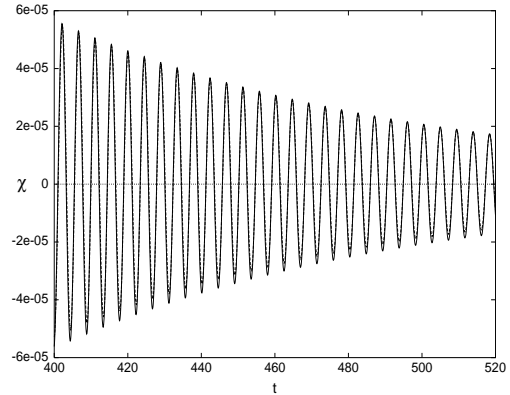


FIG. 20. The same  $\chi$  evolution at late times  $t = 400, 520$  showing the excellence of the simple fit over long times and along with the results of Fig. 19, very good agreement over three decades of amplitude.

As expected from the time dependence of the envelope of the oscillations observed in Figs. 18, 19, and 20, the damping rate cannot be obtained from a simple pole analysis. Indeed the imaginary part of  $\tilde{D}^{-1}(s)$  evaluated from the numerical data does not possess a zero for *any*  $\gamma$  with  $\omega_{pl}$  fixed at 1.405, although it does decrease monotonically as  $\gamma$  is decreased, thus favoring  $\gamma < 0.003v$ . This value is close to our momentum resolution  $dk$  and hence we could not go to lower values reliably. In any case, the decay of the envelope at late times is due to the creation of very low momentum massless bosons which have not yet dephased efficiently. Hence it is the behav-

ior of the Laplace transform on the branch cut very close to  $s = 0$  which determines the late time damping, and this behavior depends in turn on the the mode functions  $|f_k(t)|^2$  near  $k = 0$  where neither our replacement, (5.22) nor our single pole dominance assumptions are justified.

In earlier studies of damping a  $-\frac{3}{2}$  power law was encountered and identified as due to the behavior of the relevant spectral density function near threshold [24]. In the present case there is no simple argument that we are aware of which would lead to such a power law at late times.

## VII. SUMMARY

In this paper we have presented a study of nonequilibrium evolution and time dependent behavior of symmetry breaking transitions in  $N$  component  $\lambda\Phi^4$  field theory. Starting from an effective action principle for the leading order mean field approximation we emphasized the correspondence of the equations with the Schrödinger evolution of a Gaussian density matrix according to a certain effective classical Hamiltonian. This is important for emphasizing that no fundamental irreversible behavior has been introduced by the mean field approximation. Explicit numerical time evolutions from the unstable spinodal region show effective time irreversibility in the form of the efficient averaging to zero of the phase information in the density matrix. The effective von Neumann entropy of the reduced density matrix measures the information that is lost by discarding this phase information. Its general increase with particle creation shows the close connection between dephasing and irreversibility. Thus our study of effective dissipation and decoherence casts some light on fundamental issues in quantum statistical mechanics such as the origin of irreversibility, Boltzmann's H-theorem and the quantum to classical transition. Here there is much that could be done still in the context of the framework presented in this paper, most notably to study quantitatively the Poincaré recurrence cycle(s) expected in a Hamiltonian system and their dependence on the various parameters of the model.

In the specific case at hand,  $\Phi^4$  field theory is a prototype of models of of spontaneous symmetry breaking in a wide variety of physical systems. It has been common to rely heavily on the thermodynamic free energy and equilibrium considerations generally in analyzing these systems. One broad and generally applicable conclusion of the present study is that this can be very misleading where nonequilibrium dynamics is concerned. We have shown that the distribution of particles created in the mean field time evolution from an initial configuration in the spinodal region is generally far from thermal. This leads to a final state in which the mean field need not be close to minimum of the free energy potential. The simple observation that there is a sum rule which the non-thermally distributed particles can saturate is sufficient

to resolve this seemingly paradoxical result.

The linear response analysis of the oscillations about the allowed stationary configurations is also a new result which is quite different from what consideration of the free energy function alone might lead one to expect. We have shown that there is a collective plasma mode in the radial symmetry breaking direction whose characteristics depend on the ambient particle distribution. This also should be generally true of the various systems described by the same  $\Phi^4$  field theory. While there is excellent agreement in the thermal case for both the plasmon frequency and damping rate, the non-thermal situation is more complicated. In this case, due to the lack of pole dominance, the late time behavior cannot be described by exponentially damped oscillations. Our numerical results for the plasmon oscillation envelope are remarkably well-fitted by an expression of the form  $t^{-\alpha} \exp(-\gamma t)$ . The plasmon frequency compares well with an analytical estimate. However, the precise dependence of the envelope function on the particle density in the general case remains to be more fully investigated. We have outlined also how dephasing leads also to effectively classical field configurations which one can sample in order to extract information on the creation of topological defects during the phase transition. This direction is certainly an interesting one to pursue both in the condensed matter and cosmological applications.

Throughout the paper we have endeavored to bring the theoretical framework into close contact with practical numerical methods. Indeed one of the main conclusions of this work is that the real time dynamics of phase transitions can be studied in a concrete way with presently available computers. Besides the wide applicability of the spontaneously broken  $\Phi^4$  theory it is interesting for the existence of massless Goldstone bosons which are created freely during the phase transition. This essential kinematics is shared by systems with an exact gauge symmetry such as QCD or general coordinate invariance such as gravity. The numerical techniques used in this work and the experience gained in treating the massless case should prove to be valuable in generalizations to these cases.

## ACKNOWLEDGMENTS

Numerical computations were carried out on the CM5 at the Advanced Computing Laboratory, Los Alamos National Laboratory.

- 
- [1] F. Cooper, S. Habib, Y. Kluger, E. Mottola, J. P. Paz, and P. R. Anderson, *Phys. Rev. D* **50**, 2848 (1994), and references therein.

- [2] E. J. Weinberg and A. Wu, *Phys. Rev. D* **36**, 2474 (1987).  
[3] D. Boyanovsky, H. J. de Vega, R. Holman, and J. F. J. Salgado, hep-ph/9608205.  
[4] N. D. Mermin and H. Wagner, *Phys. Rev. Lett.* **17**, 1133 (1966); S. Coleman, *Comm. Math. Phys.* **31**, 259 (1973).  
[5] S. Habib, Y. Kluger, E. Mottola, and J. P. Paz, *Phys. Rev. Lett.* **76**, 4660 (1996).  
[6] Discussions of the large  $N$  method are given in, *e.g.*, S. Coleman, R. Jackiw, and H. D. Politzer, *Phys. Rev. D* **10**, 2491 (1974), R. Root, *Phys. Rev. D* **11**, 831 (1975); C. M. Bender, F. Cooper, and G. S. Guralnik, *Ann. Phys.* **109**, 165 (1977); C. M. Bender and F. Cooper, *Ann. Phys.* **160**, 323 (1985).  
[7] F. Cooper, J. Dawson, S. Habib, Y. Kluger, D. Meredith, and H. Shepard, *Physica D* **83**, 74 (1995).  
[8] F. Cooper, S.-Y. Pi, and P. Stancioff, *Phys. Rev. D* **34**, 3831 (1986).  
[9] F. Cooper and E. Mottola, *Phys. Rev. D* **36**, 3114 (1987).  
[10] A. K. Rajagopal and J. T. Marshall, *Phys. Rev. A* **26**, 2977 (1982), where the pure state case  $\sigma = 1$  only is considered.  
[11] An alternative variational approach is taken in O. J. P. Eboli, R. Jackiw, and S. Y. Pi, *Phys. Rev. D* **37**, 3557 (1988).  
[12] R. Jackiw, *Physica A* **158**, 269 (1989).  
[13] D. Kirzhnits and A. Linde, *Phys. Lett.* **42B**, 471 (1972); L. Dolan and R. Jackiw, *Phys. Rev. D* **9**, 3320 (1974); S. Weinberg, *Phys. Rev. D* **9**, 3357 (1974).  
[14] See, *e.g.*, W. A. Bardeen and M. Moshe, *Phys. Rev. D* **28**, 1372 (1983).  
[15] G. Amelino-Camelia and S.-Y. Pi, *Phys. Rev. D* **47**, 2356 (1993).  
[16] An early discussion may be found in G. Baym and G. Grinstein, *Phys. Rev. D* **15**, 2897 (1977).  
[17] K. Symanzik, *Comm. Math. Phys.* **16**, 48 (1970); C. M. Bender and F. Cooper, *Nucl. Phys.* **B224**, 403 (1983); Y. Fujimoto, L. O’Raifeartaigh, G. Parravicini, *Nucl. Phys.* **B212**, 268 (1983).  
[18] S. Weinberg *Quantum Theory of Fields, Vol. 2* (Cambridge University Press, Cambridge, 1996).  
[19] D. Boyanovsky, H. J. de Vega, R. Holman, D. S. Lee, and A. Singh, *Phys. Rev. D* **51**, 4419 (1995).  
[20] See, *e.g.*, H. Goldstein, *Classical Mechanics* (Addison-Wesley, 1980).  
[21] B. L. Hu and D. Pavon, *Phys. Lett.* **180B**, 329 (1986); H. E. Kandrup, *Phys. Rev. D* **37**, 3305 (1988); *ibid.* **38**, 1773 (1988).  
[22] E. Calzetta and B. L. Hu, *Phys. Rev. D* **40**, 656 (1989); *ibid.* **49**, 6636 (1994).  
[23] Y. Kluger, J. M. Eisenberg, B. Svetitsky, F. Cooper, and E. Mottola, *Phys. Rev. D* **45**, 4659 (1992).  
[24] D. Boyanovsky, M. D’Attanasio, H. J. de Vega, R. Holman, and D. S. Lee, *Phys. Rev. D* **52**, 5516 (1995).  
[25] S. M. Christensen, *Phys. Rev. D* **14**, 2490 (1976); *ibid.* **17**, 946 (1978).  
[26] C. G. Callan, S. Coleman, and R. Jackiw, *Ann. Phys.* **59**, 42 (1970).  
[27] L. S. Brown and J. C. Collins, *Ann. Phys.* **130**, 215 (1980).  
[28] R. G. Littlejohn, *Phys. Rep.* **138**, 193 (1986).  
[29] L. S. Brown and S. J. Carson, *Phys. Rev. A* **20**, 2486 (1979).

## APPENDIX A: THE ENERGY-MOMENTUM TENSOR AND ITS RENORMALIZATION

The effective action (2.7) leads directly to a conserved energy-momentum tensor at any order of the large  $N$  expansion [1]. In this Appendix we give some details about the energy-momentum tensor and its renormalization. Because of spatial homogeneity and isotropy the only nontrivial components of this tensor are

$$\begin{aligned}\langle T_{00} \rangle &= \varepsilon & \text{and} \\ \langle T_{ij} \rangle &= p \delta_{ij},\end{aligned}\tag{A1}$$

where the energy density  $\varepsilon$  and isotropic pressure  $p$  are given by

$$\begin{aligned}\varepsilon &= \frac{1}{2} \dot{\phi}^2 + \frac{1}{2} \chi \phi^2 - \frac{\chi}{\lambda} \left( \frac{\chi}{2} + \mu^2 \right) \\ &\quad + \frac{1}{2} \int [d\mathbf{k}] \sigma_k \left\{ |\dot{f}_k|^2 + (k^2 + \chi) |f_k|^2 \right\} \\ &= \frac{1}{2} \dot{\phi}^2 + \frac{1}{2\lambda\Lambda} \chi^2 + \frac{1}{4\pi^2} \int_0^\Lambda k^2 dk \sigma_k \left( |\dot{f}_k|^2 + k^2 |f_k|^2 \right),\end{aligned}\tag{A2}$$

and

$$\begin{aligned}p &= \frac{1}{2} \dot{\phi}^2 - \frac{1}{2} \chi \phi^2 + \frac{\chi}{\lambda} \left( \frac{\chi}{2} + \mu^2 \right) \\ &\quad + \frac{1}{2} \int [d\mathbf{k}] \sigma_k \left\{ |\dot{f}_k|^2 - \left( \frac{k^2}{3} + \chi \right) |f_k|^2 \right\} \\ &= \frac{1}{2} \dot{\phi}^2 - \frac{1}{2\lambda\Lambda} \chi^2 + \frac{1}{4\pi^2} \int_0^\Lambda k^2 dk \sigma_k \left( |\dot{f}_k|^2 - \frac{k^2}{3} |f_k|^2 \right).\end{aligned}\tag{A3}$$

We have used the gap equation (2.32) in passing to the latter expressions in each case.

The energy-density  $\varepsilon$  contains a quartic but constant cut-off dependence (*i.e.* proportional to  $\Lambda^4$ ). This is the expected vacuum energy contribution which should be subtracted. The conservation of the energy density,

$$\dot{\varepsilon} = 0\tag{A4}$$

is easily checked from the equations of motion, and is not affected by the subtraction of the constant quartic divergence. As it will turn out this single constant subtraction is sufficient to yield a cut-off independent conserved energy density.

The cut-off dependence of the isotropic pressure  $p$  is a bit more complicated and requires a detailed understanding of how Lorentz invariance (or more generally, coordinate invariance) is broken by the spatial momentum cut-off we have introduced in all the mode integrations. In the first forms of the two expressions (A2) and (A3), *i.e.* before using the gap equation, there appear mode integrals whose cut-off dependences correspond to those of a free theory with the mass  $m^2$  replaced by  $\chi(t)$ .

Divergences in the energy-momentum tensor expectation value  $\langle T_{\mu\nu} \rangle$  have been studied in the literature by covariant methods such as dimensional regularization or covariant point splitting [25] with the result that these divergences must be proportional either to the metric tensor  $g_{\mu\nu} = \text{diag}(-1, 1, 1, 1)$  in flat Minkowski spacetime or the total derivative “improvement term” of Eqn. (A12) below. Because we are using a regulator in the form of a cut-off in the spatial momentum integrations which is *not* covariant under Lorentz or general time dependent coordinate transformations, the quartic and quadratic cut-off dependence we shall actually obtain will not have these covariant forms. Hence we shall have to perform the stress tensor renormalization in a noncovariant manner as well to correct for the spurious noncovariant  $\Lambda^4$  and  $\Lambda^2$  cut-off dependence, in order to obtain covariant results in the end.

The actual cut-off dependence in both  $\varepsilon$  and  $p$  is easily analyzed by means of an adiabatic expansion to the mode function equation (2.20), the lowest order solution of which is given by Eqn. (5.12). By substituting this lowest order adiabatic approximation to the mode functions into the mode integrals in the first forms of Eqns. (A2) and (A3) we can characterize the most severe dependence on the ultraviolet cut-off  $\Lambda$  in the forms,

$$\begin{aligned} \varepsilon_0 &\equiv \frac{\hbar}{4\pi^2} \int_0^\Lambda k^2 dk \sqrt{k^2 + \chi} \\ &= \frac{\hbar\Lambda^4}{16\pi^2} + \frac{\hbar\Lambda^2\chi}{16\pi^2} - \frac{\hbar\chi^2}{64\pi^2} \ln\left(\frac{4\Lambda^2}{\chi}\right) + \frac{\hbar\chi^2}{128\pi^2} + \mathcal{O}\left(\frac{\chi^3}{\Lambda^2}\right) \end{aligned} \quad (\text{A5})$$

and

$$\begin{aligned} p_0 &\equiv \frac{\hbar}{12\pi^2} \int_0^\Lambda \frac{k^4 dk}{\sqrt{k^2 + \chi}} \\ &= \frac{\hbar\Lambda^4}{48\pi^2} - \frac{\hbar\Lambda^2\chi}{48\pi^2} + \frac{\hbar\chi^2}{64\pi^2} \ln\left(\frac{4\Lambda^2}{\chi}\right) - \frac{7\hbar\chi^2}{384\pi^2} + \mathcal{O}\left(\frac{\chi^3}{\Lambda^2}\right). \end{aligned} \quad (\text{A6})$$

Clearly the  $\Lambda$  dependence is *not* such that  $\varepsilon_0 = -p_0$ , as required by considerations of general covariance. As has been known for some time the reason for this is that the spatial momentum cut-off  $\Lambda$  acts as a noncovariant point splitting regulator would, giving terms in the regulated  $\langle T_{\mu\nu} \rangle$  proportional to  $\delta_{(\mu}^i \delta_{\nu)}^j$  in which the spatial directions  $i, j = 1, 2, 3$  are distinguished. Since such terms do not appear in the  $\mu = \nu = 0$  time component, the energy density has the correct  $\Lambda$  dependence and requires no covariantizing correction. However for the pressure we should have

$$p'_0 \equiv -\varepsilon_0 \quad (\text{A7})$$

on grounds of general covariance. This is easy to enforce *by hand* by adding the difference  $p'_0 - p_0 = -\varepsilon_0 - p_0$  to  $p_0$  above which just corrects for the noncovariant terms induced by our momentum cut-off.

With this prescription to enforce covariance of the mode integrals in the pressure, the quartic subtraction required on both  $\varepsilon$  and  $p$  is the removal of the cosmological vacuum energy  $\hbar\Lambda^4/16\pi^2$ , corresponding to a subtractive renormalization of the constant cosmological vacuum term. We are *not* allowed to subtract the subleading quadratic and logarithmic divergences of  $\varepsilon$  appearing in Eqn. (A5), since, for one thing, they are multiplied by the time dependent function  $\chi$  and hence would spoil energy conservation, and for another, such time dependent terms do not correspond to a constant vacuum energy. Instead we recognize them to be just the correct cut-off dependent terms needed to combine with the cut-off dependent terms in the “classical” energy density,

$$\begin{aligned} -\frac{\chi}{\lambda\Lambda} \left( \frac{\chi}{2} + \mu_\Lambda^2 \right) &= -\frac{\chi^2}{2} \left\{ \frac{1}{\lambda_R(m^2)} - \hbar \frac{1}{32\pi^2} \ln\left(\frac{4\Lambda^2}{m^2}\right) \right\} \\ &\quad - \chi \left( \frac{v^2}{2} + \frac{\hbar\Lambda^2}{16\pi^2} \right) \end{aligned} \quad (\text{A8})$$

in order to render the total energy density cut-off independent. Because the analogous terms in  $p$  are precisely the negative of those appearing in  $\varepsilon$  after the correction  $p'_0 - p_0$  has been added to its quantum part, we also obtain a (partially) renormalized pressure by the same manipulations.

The reason that we must still perform one additional subtraction to obtain a fully renormalized pressure is that at the next order in the WKB adiabatic expansion of the mode equation (2.20), one obtains for the adiabatic frequency,

$$\omega_k \rightarrow \omega_k - \frac{1}{4} \frac{\ddot{\omega}_k}{\omega_k^2} + \frac{3}{8} \frac{\dot{\omega}_k^2}{\omega_k^3} + \dots \quad (\text{A9})$$

If the energy density is calculated to this adiabatic order one finds no additional cut-off dependence in  $\varepsilon$ , so no additional subtractions are required for it. Indeed none are permitted consistent with the principle of general coordinate invariance. However, the pressure has an additional logarithmic cut-off dependence equal to

$$-\frac{\hbar}{96\pi^2} \ddot{\chi} \ln\left(\frac{4\Lambda^2}{\chi}\right). \quad (\text{A10})$$

Since this divergence appears only in the pressure but not in the energy it is consistent with the generally covariant and conserved form of the “improvement term,” [26]

$$\Delta\langle T_{\mu\nu} \rangle = \xi(g_{\mu\nu}\square - \partial_\mu\partial_\nu)\langle\Phi^2\rangle \quad (\text{A11})$$

in flat space. This term has no effect on the energy density for spatially homogeneous mean fields but adds to the pressure the total derivative,

$$\Delta p = -\xi \frac{d^2}{dt^2} \left\{ \phi^2 + \int [d^3\mathbf{k}] \sigma_k |f_k|^2 \right\} = -2\frac{\xi}{\lambda} \ddot{\chi} \quad (\text{A12})$$

in which  $\xi$  is an arbitrary parameter. The fact that a divergence such as (A10) appears in the pressure means

that we should introduce  $\xi$  as a free bare parameter of the theory from the very beginning, on the same footing as the mass  $\mu_\Lambda^2$  and coupling  $\lambda_\Lambda$ , and allow for the possibility that the bare  $\xi_\Lambda \neq 0$  will renormalize in general. Indeed this is known to be the case in  $\lambda\Phi^4$  theory [27] and we have the renormalization condition,

$$\left(\xi_\Lambda - \frac{1}{6}\right) = Z_\lambda^{-1}(\Lambda, m) \left(\xi_R(m^2) - \frac{1}{6}\right) \quad (\text{A13})$$

where  $Z_\lambda^{-1}$  is the same logarithmic renormalization constant as that for the coupling constant appearing in Eqns. (2.35) and (2.36) of the text. Thus,

$$\frac{\xi_\Lambda}{\lambda_\Lambda} = \frac{1}{6\lambda_\Lambda} + \frac{1}{\lambda_R} \left(\xi_R - \frac{1}{6}\right) \quad (\text{A14})$$

and the additional term in the pressure (A12) becomes

$$\begin{aligned} \Delta p &= -\frac{1}{3\lambda_\Lambda} \ddot{\chi} - \frac{2}{\lambda_R} \left(\xi_R - \frac{1}{6}\right) \ddot{\chi} \\ &= +\frac{1}{96\pi^2} \ln\left(\frac{4\Lambda^2}{m^2}\right) \ddot{\chi} - \frac{2\xi_R}{\lambda_R} \ddot{\chi}. \end{aligned} \quad (\text{A15})$$

Comparing the latter expression with (A10) we observe that the logarithmic cut-off dependence cancels in the sum  $p + \Delta p$ . Hence we *must* add the improvement term and renormalize  $\xi$  in precisely this way in order to obtain a completely cut-off independent pressure.

To summarize this discussion of the renormalization of the energy and pressure we define

$$\varepsilon_R = \varepsilon - \frac{\hbar\Lambda^4}{16\pi^2} \quad (\text{A16})$$

to be the cut-off independent conserved energy density, and

$$p_R = p - p_0 - \varepsilon_0 + \frac{\hbar\Lambda^4}{16\pi^2} + \Delta p \quad (\text{A17})$$

to be the renormalized pressure of the  $\Phi^4$  theory for the spatially homogeneous mean fields considered in this paper.

Let us also remark that the value  $\xi = 1/6$  for the improvement term is also the value chosen for conformal invariance of the scalar theory in the massless limit. Indeed the trace of the renormalized energy-momentum tensor is

$$\begin{aligned} \langle T^\mu{}_\mu \rangle_R &= -\varepsilon_R + 3p_R \\ &= v^2\chi + \frac{\hbar\chi^2}{32\pi^2} + \frac{1}{\lambda_R} \left(\xi_R - \frac{1}{6}\right) \ddot{\chi} \end{aligned} \quad (\text{A18})$$

upon using Eqns. (A5), (A6), and (A15) above. At  $\xi = 1/6$  the last term vanishes, the first term is the renormalized classical trace of the energy-momentum tensor and the second term is the one-loop quantum trace anomaly,

$$\frac{1}{2\lambda_R^2} \beta(\lambda_R) \chi^2 = -\frac{\chi^2}{2} \Lambda \frac{d}{d\Lambda} \left(\frac{1}{\lambda_\Lambda}\right) = \frac{\hbar\chi^2}{32\pi^2} \quad (\text{A19})$$

in terms of the  $\beta$  function of the coupling constant  $\lambda$ . We note that the trace of the renormalized energy momentum tensor vanishes (for any value of  $\xi$ ) in the static spontaneously broken vacuum where  $\dot{\phi} = \chi = 0$  and

$$f_k = \sqrt{\frac{\hbar}{2k}} e^{-ikt}.$$

This implies that the relativistic equation of state

$$p_R \rightarrow \frac{1}{3} \varepsilon_R \quad (\text{A20})$$

holds at late times, independently of the number density distribution. The numerically obtained approach to this equation of state is shown in Fig. 20. We emphasize that this equation of state does not imply relaxation to thermal equilibrium since collisional effects are not yet taken into account by the leading order large  $N$  approximation, and the nonthermal nature of the late time state is apparent from the created particle distribution of Fig. 10.

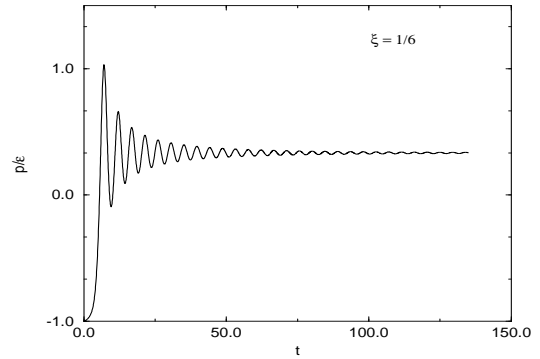


FIG. 21. Evolution of the pressure as a function of time for  $\xi = 1/6$ . The approach to the equation of state  $p = \varepsilon/3$  is clearly seen.

## APPENDIX B: THE GAUSSIAN DENSITY MATRIX $\rho$

In this second Appendix we examine some of the properties of the general mixed state Gaussian density matrix (3.16) and its time evolution. The discussion will be restricted mainly to the case of  $d = 0$  spatial dimensions to simplify the notation. Generalizations to  $d > 0$  are straightforward. First, the time evolution of the density matrix is unitary:

$$\rho(t) = U(t)\rho(0)U^\dagger(t), \quad U(t) = \exp\left(-i \int_0^t H_{osc} dt\right), \quad (\text{B1})$$

where  $H_{osc}$  is the time-dependent harmonic oscillator Hamiltonian,

$$H_{osc}(\Phi, \mathbf{P}; t) \equiv \frac{1}{2} (\mathbf{P}^2 + \omega^2(t) \Phi^2) \quad (\text{B2})$$

that preserves the Gaussian structure of  $\rho$  under time evolution, so that the Liouville equation,

$$i\hbar \frac{\partial}{\partial t} \rho = [H_{osc}, \rho] \quad (\text{B3})$$

is satisfied without taking the trace.

It is not difficult to find the explicit form of the unitary operator  $U(t)$  in the coordinate basis,

$$\begin{aligned} \langle x' | U(t) | x \rangle &= (2\pi i \hbar v(t))^{-\frac{1}{2}} \times \\ &\exp \left\{ \frac{i}{2\hbar v(t)} (u(t)x^2 + \dot{v}(t)x'^2 - 2xx') \right\} \end{aligned} \quad (\text{B4})$$

in terms of the two linearly independent solutions to the classical evolution equation,

$$\left( \frac{d^2}{dt^2} + \chi^2(t) \right) \begin{pmatrix} u \\ v \end{pmatrix} = 0; \quad \begin{aligned} u(0) &= \dot{v}(0) = 1 \\ \dot{u}(0) &= v(0) = 0 \end{aligned} \quad (\text{B5})$$

This same  $U(t)$  also evolves the quantum operators,

$$\begin{aligned} \Phi(t) &= U^\dagger(t) \Phi(0) U(t) = \phi(t) + af(t) + a^\dagger f^*(t) \\ \mathbf{P}(t) &= U^\dagger(t) \mathbf{P}(0) U(t) = p(t) + a\dot{f}(t) + a^\dagger \dot{f}^*(t) \end{aligned} \quad (\text{B6})$$

Mathematically, the three Fock space bilinear operators  $aa$ ,  $a^\dagger a^\dagger$  and  $a^\dagger a + aa^\dagger$  generate the Lie algebra of the symplectic group  $Sp(2) \cong SU(1, 1) \cong SL(2, R)$  which is the group of homogeneous linear transformations of phase space  $(\Phi, \mathbf{P})$  which preserves the anti-symmetric classical Poisson bracket  $\{\Phi, \mathbf{P}\} = 1$ , *i.e.*

$$\begin{pmatrix} \Phi \\ \mathbf{P} \end{pmatrix} \rightarrow \begin{pmatrix} \Phi' \\ \mathbf{P}' \end{pmatrix} = \begin{pmatrix} a & b \\ c & d \end{pmatrix} \begin{pmatrix} \Phi \\ \mathbf{P} \end{pmatrix} \quad (\text{B7})$$

with

$$ab - cd = 1. \quad (\text{B8})$$

Since this is one condition on four real parameters the group  $Sp(2)$  is a three parameter group. If the  $a$  and  $a^\dagger$  Heisenberg operators are appended to these three, the algebra again closes upon itself, forming a five parameter group, the inhomogeneous metaplectic group,  $IMp(2)$  [28]. The unitary evolution (B1), (B4) of the Gaussian density matrix (3.16) is an explicit representation of this group's action.

The form of the density matrix in the time-independent Heisenberg basis is quite easy to obtain from the form of the transition matrix element  $\langle x | n \rangle$  given by Eqn. (5.7) of the text. By substituting the integral representation of the Hermite polynomials,

$$H_n(x) = \frac{n!}{2\pi i} \oint_{\mathcal{C}} \frac{dz}{z^{n+1}} e^{2xz - z^2} \quad (\text{B9})$$

where  $\mathcal{C}$  is a closed contour around the origin of the complex  $z$  plane into the expression

$$\langle n' | \rho | n \rangle = \int_{-\infty}^{\infty} dx' \int_{-\infty}^{\infty} dx \langle n' | x' \rangle \langle x' | \rho | x \rangle \langle x | n \rangle \quad (\text{B10})$$

and interchanging the orders of integration we can perform the double Gaussian integral over the shifted vector  $(x - \phi, x' - \phi)$  first. Using the standard formula

$$\int_{-\infty}^{\infty} d^2x e^{-x \cdot A \cdot x + B \cdot x} = \frac{\pi}{(\det A)^{\frac{1}{2}}} e^{\frac{1}{4} B^T \cdot A^{-1} \cdot B} \quad (\text{B11})$$

with  $A$  the  $2 \times 2$  matrix

$$A = \frac{\sigma + 1}{8\xi^2} \begin{pmatrix} 1 + \sigma & 1 - \sigma \\ 1 - \sigma & 1 + \sigma \end{pmatrix} \quad (\text{B12})$$

and  $B$  the column vector

$$B = \frac{\sqrt{2\sigma}}{\xi} \begin{pmatrix} z \\ z'^* \end{pmatrix} \quad (\text{B13})$$

the exponent of the resulting expression simplifies considerably. Letting  $z = e^{i\theta}$  and  $z'^* = e^{-i\theta'}$  we are left with

$$\begin{aligned} \langle n' | \rho | n \rangle &= \frac{2}{\sigma + 1} \left( \frac{n'! n!}{2^{n'+n}} \right)^{\frac{1}{2}} \times \\ &\int_0^{2\pi} \frac{d\theta'}{2\pi} e^{in'\theta'} \int_0^{2\pi} \frac{d\theta}{2\pi} e^{-in\theta} \exp \left\{ 2 \left( \frac{\sigma - 1}{\sigma + 1} \right) e^{i(\theta - \theta')} \right\}. \end{aligned} \quad (\text{B14})$$

Expanding the last exponent in a Taylor series we find that only the terms with  $n' = n$  survive with Eqn. (5.8) the final result. As discussed earlier in Section VI, in this Heisenberg basis the density matrix is time-independent and diagonal. This fact allows the writing of (B14) in an operator form,

$$\bar{\rho} = \frac{2}{\sigma + 1} \exp \left\{ \ln \left( \frac{\sigma - 1}{\sigma + 1} \right) a^\dagger a \right\} \quad (\text{B15})$$

as far as computing matrix elements in this Heisenberg basis is concerned.

By making a different  $IMp(2)$  group transformation it is also possible to diagonalize (B2) at any given time, bringing the quadratic Hamiltonian into the standard harmonic oscillator form,  $H_{osc} = \frac{\hbar\omega}{2} (\tilde{a}\tilde{a}^\dagger + \tilde{a}^\dagger\tilde{a})$  with  $\tilde{a}$  time dependent. This adiabatic particle basis is related to the time-independent Heisenberg basis by the relations,

$$\begin{aligned} f &= \alpha \tilde{f} + \beta \tilde{f}^*, \\ a &= \alpha^* \tilde{a} - \beta^* \tilde{a}^\dagger + \kappa^* \end{aligned} \quad (\text{B16})$$

with  $\tilde{f}$  the adiabatic mode function defined by Eqn. (5.12) of the text, and

$$\begin{aligned}\alpha &= \frac{i}{\hbar} \tilde{f}^* (\dot{f} - i\omega f), \\ \beta &= -\frac{i}{\hbar} \tilde{f} (\dot{f} + i\omega f), \\ \kappa &= \frac{i}{\hbar} (\dot{\phi} f - \phi \dot{f}).\end{aligned}\quad (\text{B17})$$

The Bogoliubov coefficients  $\alpha$  and  $\beta$  obey

$$|\alpha|^2 - |\beta|^2 = 1 \quad (\text{B18})$$

and therefore may be expressed in terms of a real parameter  $\gamma$  and two phases,

$$\begin{aligned}\alpha &= \cosh \gamma e^{i\psi}, \\ \beta &= -\sinh \gamma e^{i(\psi-\theta)}.\end{aligned}\quad (\text{B19})$$

The density matrix in the adiabatic particle number basis can be expressed in terms of these time dependent parameters at any given time  $t$ . The direct evaluation of the expression analogous to (B10) in the  $\tilde{n}$  number basis is quite tedious, and is accomplished most rapidly by use of a coherent state basis as discussed in Ref. [29]. Making the identifications,

$$\begin{aligned}\alpha &= \frac{1}{S_{-+}^*} = \frac{S_{+-}}{1 - |S_{++}|^2}, \\ \beta &= \frac{S_{--}}{S_{-+}} = -\frac{S_{+-} S_{++}^*}{1 - |S_{++}|^2}\end{aligned}\quad (\text{B20})$$

with

$$\begin{aligned}S_{+-} &= S_{-+} = \text{sech} \gamma e^{i\psi}, \\ S_{++} &= \tanh \gamma e^{i\theta}, \\ S_{--} &= -\tanh \gamma e^{2i\psi - i\theta}\end{aligned}\quad (\text{B21})$$

and  $\chi \rightarrow \gamma$  in the notation of Ref. [29], Eqn. (5.32) of that work yields the desired matrix element in the case of zero mean field, namely,

$$\begin{aligned}\langle \tilde{n}' | \rho | \tilde{n} \rangle \Big|_{\phi=0} &= 2e^{\frac{i}{2}(\tilde{n}' - \tilde{n})\theta} \left( \frac{\tilde{n}'!}{\tilde{n}!} \right)^{\frac{1}{2}} \times \\ &[(\sigma^2 - 1)^2 - 4\sigma^2 \sinh^2 2\gamma]^{\frac{1}{4}(\tilde{n}' + \tilde{n})} \times \\ &[\sigma^2 + 1 + 2\sigma \cosh 2\gamma]^{-\frac{1}{4}(\tilde{n}' + \tilde{n} + 1)} \times \\ &P_{\frac{1}{2}(\tilde{n} - \tilde{n}')}^{\frac{1}{2}(\tilde{n} + \tilde{n}')} \left( \left[ 1 - \frac{4\sigma^2}{(\sigma^2 - 1)^2} \sinh^2 2\gamma \right]^{-\frac{1}{2}} \right),\end{aligned}\quad (\text{B22})$$

where  $P_n^m$  is an associated Legendre polynomial.

The first important feature of this expression for our purposes is the phase factor when  $\tilde{n} \neq \tilde{n}'$ . If the exact mode function  $f$  is rewritten in the form

$$f(t) = \sqrt{\frac{\hbar}{2\Omega(t)}} \exp \left( -i \int_0^t dt' \Omega(t') \right), \quad (\text{B23})$$

this phase

$$\begin{aligned}\theta &= \arg \left( \frac{\alpha}{-\beta} \right) \\ &= 2 \int_0^t dt' \omega(t') + \tan^{-1} \left( \frac{\frac{\dot{\Omega}\omega}{\Omega}}{\Omega^2 - \omega^2 + \frac{\dot{\Omega}^2}{4\Omega^2}} \right).\end{aligned}\quad (\text{B24})$$

Thus, even in the adiabatic limit, where  $\frac{\dot{\Omega}}{\Omega^2} \ll 1$ , the phase angle  $\theta$  depends linearly on time and the off-diagonal elements of the density matrix (B22) are rapidly varying in time. On the other hand, the diagonal elements of (B22) are independent of this phase angle and consequently much more slowly varying functions of time. Indeed, in the case of zero mean field  $\phi = 0$ , the adiabatic invariant  $W$  of Eqn. (5.20) is

$$W = \tilde{N} - N = \sigma \sinh^2 \gamma \quad (\text{B25})$$

and  $\langle \tilde{n} | \rho | \tilde{n} \rangle$  depends only upon  $\sigma$  (a constant) and  $\gamma$ :

$$\begin{aligned}\langle \tilde{n} | \rho | \tilde{n} \rangle &= 2 [(\sigma^2 - 1)^2 - 4\sigma^2 \sinh^2 2\gamma]^{\frac{1}{2}\tilde{n}} \\ &\times [\sigma^2 + 1 + 2\sigma \cosh 2\gamma]^{-\frac{1}{4}(2\tilde{n}+1)} \\ &\times P_{\tilde{n}} \left( \left[ 1 - \frac{4\sigma^2}{(\sigma^2 - 1)^2} \sinh^2 2\gamma \right]^{-\frac{1}{2}} \right)\end{aligned}\quad (\text{B26})$$

Now if  $\sigma > 1$  the Legendre polynomial is not necessarily positive which means that we cannot interpret the diagonal matrix elements of the density matrix in the adiabatic particle number basis as a classical probability distribution in the general mixed state case. However, if  $\sigma = 1$  then the argument of the Legendre polynomial vanishes for any  $\gamma \neq 0$ . Since

$$P_{2\ell}(0) = (-1)^\ell \frac{(2\ell - 1)!!}{2^\ell \ell!} \quad (\text{B27})$$

for  $\tilde{n} = 2\ell$  even but  $P_{2\ell+1}(0) = 0$  for  $\tilde{n} = 2\ell + 1$  odd, the diagonal matrix element (B26) simplifies considerably in the pure state case,

$$\langle \tilde{n} = 2\ell | \rho | \tilde{n} = 2\ell \rangle \Big|_{\substack{\sigma=1 \\ \phi=\phi=0}} = \frac{(2\ell - 1)!!}{2^\ell \ell!} \text{sech} \gamma \tanh^{2\ell} \gamma \quad (\text{B28})$$

with the mean number of created particles,

$$\tilde{N} = \sinh^2 \gamma = \frac{|\dot{f} + i\omega f|^2}{2\hbar\omega}, \quad (\text{B29})$$

which are Eqns. (5.25) and (5.26) of the text. These results were reported in [5].

In the pure state case the even  $\tilde{n}$  diagonal matrix elements of the density matrix are positive definite and may be interpreted as the probabilities for observing  $\ell$  uncorrelated particle pairs in the adiabatic particle basis. The odd  $\tilde{n}$  diagonal matrix elements vanish since particles can

only be created in pairs from the vacuum. Otherwise (*i.e.* for  $\sigma > 1$ ), the much more complicated and non-positive definite expression (B26) shows that there is no simple classical probability interpretation for the density matrix. The restriction to zero mean fields  $\phi = \dot{\phi} = 0$  is not serious for spatially homogeneous backgrounds because of Eqn. (3.31) which shows that all the mean fields vanish except for the  $k = 0$  mode. Hence, at late times all the  $k > 0$  modes may be treated classically if dephasing is effective and typical classical field configurations in the ensemble can be constructed as in Eqns. (5.30) and (5.31) of the text, provided the  $k = 0$  mode is excluded.

### APPENDIX C: NUMERICAL METHODS

In order to solve the system of equations (2.15), (2.20), and (2.34) as an initial value problem, we have to specify the initial conditions of the mean field  $\phi$ , its time derivative and the mode function and its time derivative. Then we have to solve the gap equation (2.34) at the initial time  $t_0$ . In order to have a finite set of renormalized equations we have to choose the mode functions so that the high momentum modes coincide with the zeroth order adiabatic vacuum described by

$$f_k(t_0) = \frac{1}{\sqrt{2\omega_k(t_0)}} , \quad (\text{C1})$$

$$\dot{f}_k(t_0) = \left[ -i\omega_k(t_0) - \frac{\dot{\omega}_k(t_0)}{2\omega_k(t_0)} \right] f_k(t_0) , \quad (\text{C2})$$

with  $\omega_k^2(t_0) = k^2 + \chi(t_0)$ . It is easy to verify that for initial conditions with  $\dot{\phi}(t_0) = 0$ , it is also true that  $\dot{\chi}(t_0) = 0$  by inspecting the time derivative of the gap equation. This simplifies the form of  $\dot{f}_k(t_0)$  to

$$\dot{f}_k(t_0) = -i\omega_k(t_0)f_k(t_0) . \quad (\text{C3})$$

For an initial state with positive square effective mass  $\chi$  we could use the same form of the mode functions of (C1) also for the low momentum modes. However, if we wish to investigate the case of a “quench” within the unstable spinodal region by initial conditions with a negative  $\chi(0)$ , we have to modify the initial values of the low momentum modes in order to avoid the singularity of  $f_k(t_0) = 1/\sqrt{2\omega_k}$  at  $k^2 = -\chi(t_0)$ . We have used two different profiles of the frequency  $\omega_k$  for the initial mode functions:

$$\omega_k^2(t_0) = k^2 + \chi(t_0) \tanh \left( \frac{k^2 + \chi(t_0)}{|\chi(t_0)|} \right) , \quad (\text{C4})$$

$$\omega_k^2(t_0) = k^2 + \chi(t_0) \exp(-v^4/k^4) . \quad (\text{C5})$$

At large momentum these profiles coincide with the adiabatic vacuum frequency as required. In all cases, except for thermal initial conditions, the initial number of quasi-particles,  $N(k) = 0$ .

Numerical simulations were performed on a massively parallel computer using a momentum grid with 32000 modes. The upper cut-off was set at  $\Lambda = 5v$ , implying a grid resolution:

$$dk = \frac{\Lambda}{32000} .$$

The field  $\phi$  was scaled in units of  $v$  so that  $k$  is also given in units of  $v$ ,  $\chi$  in units of  $v^2$ , and the time  $t$  in units of  $v^{-1}$ . Most of the results discussed here are for a bare coupling constant  $\lambda_\Lambda = 1$  but other values were also investigated. The corresponding renormalized coupling constants at the renormalization point  $|\chi(t_0)|$  are given by (2.35) with  $m^2$  replaced by  $|\chi(t_0)|$ . With  $\lambda_\Lambda = 1$ , and for  $\phi(t_0)/v = 0$ ,  $\lambda_R = 0.990036$ , while for  $\phi(t_0)/v = 0.5$ ,  $\lambda_R = 0.990248$ . The energy densities in these cases are  $\varepsilon = 0.1237$  and  $\varepsilon = 0.06978$  respectively.

The mode equations were stepped forward in time using a sixth-order adaptive time-step Runge-Kutta integrator. The time-steps were controlled by tracking the evolution of  $\chi$ . Energy conservation to parts per million was achieved over the temporal range of typical evolutions.